



Changes in the convective population and thermodynamic environments in convection-permitting regional climate simulations over the United States

K. L. Rasmussen^{1,3} · A. F. Prein³ · R. M. Rasmussen² · K. Ikeda² · C. Liu²

Received: 12 January 2017 / Accepted: 29 October 2017 / Published online: 25 November 2017
© The Author(s) 2017. This article is an open access publication

Abstract

Novel high-resolution convection-permitting regional climate simulations over the US employing the pseudo-global warming approach are used to investigate changes in the convective population and thermodynamic environments in a future climate. Two continuous 13-year simulations were conducted using (1) ERA-Interim reanalysis and (2) ERA-Interim reanalysis plus a climate perturbation for the RCP8.5 scenario. The simulations adequately reproduce the observed precipitation diurnal cycle, indicating that they capture organized and propagating convection that most climate models cannot adequately represent. This study shows that weak to moderate convection will decrease and strong convection will increase in frequency in a future climate. Analysis of the thermodynamic environments supporting convection shows that both convective available potential energy (CAPE) and convective inhibition (CIN) increase downstream of the Rockies in a future climate. Previous studies suggest that CAPE will increase in a warming climate, however a corresponding increase in CIN acts as a balancing force to shift the convective population by suppressing weak to moderate convection and provides an environment where CAPE can build to extreme levels that may result in more frequent severe convection. An idealized investigation of fundamental changes in the thermodynamic environment was conducted by shifting a standard atmospheric profile by ± 5 °C. When temperature is increased, both CAPE and CIN increase in magnitude, while the opposite is true for decreased temperatures. Thus, even in the absence of synoptic and mesoscale variations, a warmer climate will provide more CAPE and CIN that will shift the convective population, likely impacting water and energy budgets on Earth.

1 Introduction

Clouds are a critical component of the climate system and they determine a large proportion of the water and energy budgets on Earth (Allen and Ingram 2002). However,

determining the impact of clouds on the climate system, from thin cirrus to optically thick cumulonimbus clouds that extend throughout the entire troposphere, is a great challenge given their complex interactions with radiative, thermodynamic, microphysical, and dynamic processes on Earth (Stephens and Webster 1981; Hartmann et al. 1992, 2001; Hobbs 1993; Hansen et al. 1997). In addition, assessing how clouds and precipitation may change in a future climate is challenging given that fine-scale cloud and mesoscale processes are important in determining the global nature of convection (Houze et al. 2015). Del Genio and Kovari (2002) suggest that the precipitation efficiency of convective systems increases with increasing temperatures. The cloud radiative forcing and tropical radiation budget critically depend on the cloud type (Dhuria and Kyle 1990; Hartmann and Michelsen 1993). From a theoretical perspective, it is widely recognized that cloud radiative feedback processes are likely composed of both dynamical and thermodynamical components (Bony et al. 2004) from changes in the large-scale atmospheric circulation and the thermodynamic structure of the

This paper is a contribution to the special issue on Advances in Convection-Permitting Climate Modeling, consisting of papers that focus on the evaluation, climate change assessment, and feedback processes in kilometer-scale simulations and observations. The special issue is coordinated by Christopher L. Castro, Justin R. Minder, and Andreas F. Prein.

✉ K. L. Rasmussen
kristenr@rams.colostate.edu

¹ Department of Atmospheric Science, Colorado State University, Fort Collins, CO, USA

² Research Applications Laboratory, National Center for Atmospheric Research, Boulder, CO, USA

³ Mesoscale and Microscale Meteorology Laboratory, National Center for Atmospheric Research, Boulder, CO, USA

atmosphere, respectively. However, despite the importance of clouds on the hydrological cycle and energy budget of the Earth, it is well recognized that climate models produce cloud radiative feedbacks that are notably different between models that sometimes have the opposite sign (Le Treut and McAvaney 2000; Bony et al. 2004) and do not accurately represent the seasonal or diurnal cycles of convection and precipitation (Allen and Ingram 2002).

Given the profound influence of clouds and precipitation on Earth's energy and water budgets, numerous studies have examined how precipitation will change in a future climate. Higher global temperatures will lead to increased atmospheric water vapor and thus it might be expected that precipitation will be more intense and longer lasting (Trenberth et al. 2003; Sheffield and Wood 2008; Del Genio and Kovari 2002; Pall et al. 2007; O'Gorman and Schneider 2009; Kendon et al. 2012, 2014; Prein et al. 2016). In addition, the intensity of future precipitation is estimated to increase by ~7% per degree Celsius (Trenberth et al. 2003), which is derived from the Clausius–Clapeyron relationship. However, coarse resolution climate models only predict a ~3–4% increase per degree Celsius (Allen and Ingram 2002). Prein et al. (2016) looked at hourly precipitation extremes from convection-permitting climate simulations (horizontal grid spacing ≤ 4 km) over the US (the same simulations used in this study) and found that hourly precipitation extremes increase with temperature in moist, energy-limited environments at a scaling rate of ~7% per degree Celsius. This scaling rate is consistent with the results from Ban et al. (2015) looking at heavy precipitation changes over the European Alps using convection-permitting simulations. Thus, when convection-permitting horizontal resolutions are used in regional climate simulations, the expected scaling rate from the Clausius–Clapeyron equation is obtained (Prein et al. 2016; Ban et al. 2015) and such large increases will pose great risks for flooding and hydrometeorological extremes in a warmer climate. The intensification of hourly precipitation extremes in convection-permitting simulations has also been demonstrated in the U.K. and Western Europe (Lenderink and van Meijgaard 2010; Kendon et al. 2012, 2014; Ban et al. 2015).

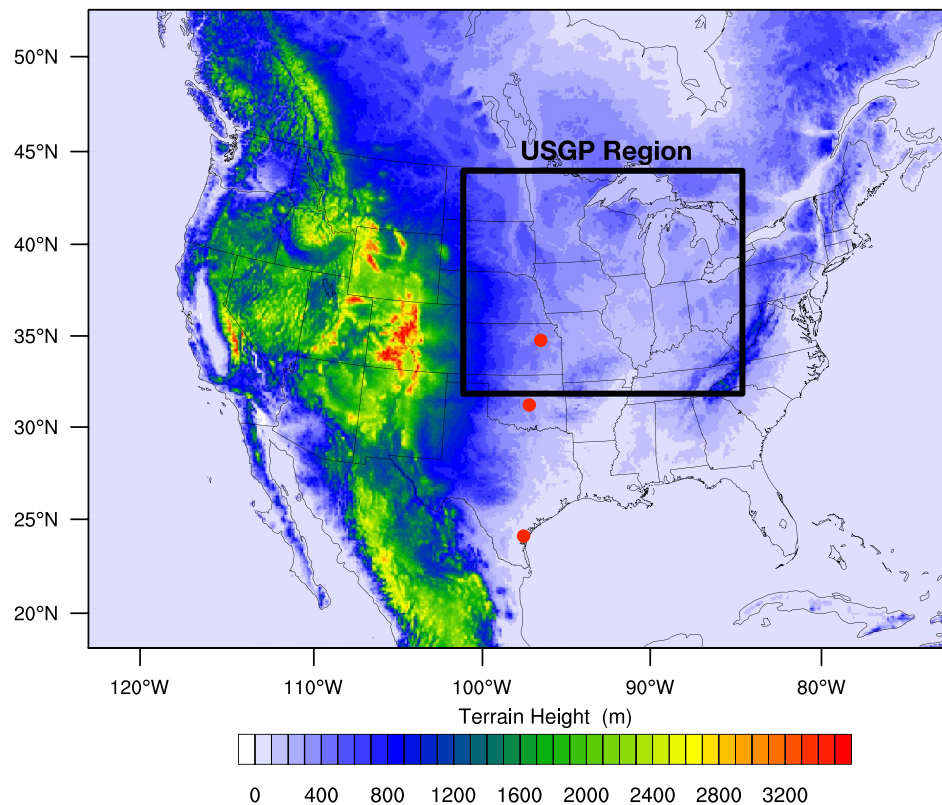
Most studies that have looked at changes in clouds and convection in a future climate have used coarse resolution climate models that may not adequately represent the fine-scale cloud and mesoscale processes critical for understanding the physical mechanisms that may result in a changing convective population (Klein and Hartmann 1993; Bony et al. 2004). Advances in computing power have resulted in numerous regional climate simulations at convection-permitting resolution around the world (Hohenegger et al. 2008; Trapp et al. 2010; Pan et al. 2011; Rasmussen et al. 2011, 2014b; Ban et al. 2015; Prein et al. 2015; Liu et al. 2016 and many others). Chan et al. (2014) showed the value

of convection-permitting simulations by comparing 12- and 1.5-km regional climate simulations using extreme value theory. They found erroneous sub-daily extreme precipitation events in the 12-km simulations because of issues with “grid point storms.”

Some recent studies have used idealized modeling frameworks to look at how convection may vary with climate change (Seeley and Romps 2015; Romps et al. 2014). Results from the idealized studies suggest that convection and severe weather are expected to increase in a warmer climate from enhanced convective available potential energy (CAPE). These results are consistent with state-of-the-art climate model simulations that suggest that future increases in hazardous convective weather are due to an increase in CAPE (Trapp et al. 2007, 2009; Diffenbaugh et al. 2013; Brooks 2013; Lackmann 2013; Gensini and Mote 2014; Trapp and Hoogewind 2016). Trapp et al. (2009) shows that decreases in synoptic disturbances affect the convective storm environment using CESM simulations. However, other studies suggest that synoptic activity may not change significantly in a future climate under the A1B scenario using the ECHAM5 model (Bengtsson et al. 2006). A few studies have used convection-permitting climate model simulations to assess future changes in convection. Gensini and Mote (2015) found a 236% increase in the frequency of grid points with CAPE exceeding 2000 J kg^{-1} in the end-of-century A2 climate projection scenario for the eastern US. Mahoney et al. (2013) downscaled current and future climate extreme event case studies from multiple driving models over Colorado and found increases of CAPE from 200 to 800 J kg^{-1} over the Colorado plains and mostly decreases over mountainous regions. This resulted in a decrease in the intensity of extreme events, even though localized maxima did increase. In general, convection-permitting climate simulations enable a more physical based representation of deep convection and its relationship to the surrounding environments with fewer parameterization-based uncertainties (Prein et al. 2015).

Partially motivated by previous studies on the nature of convection around the world (Zipser et al. 2006; Rasmussen and Houze 2011, 2016; Zuluaga and Houze 2015; Houze et al. 2015; Rasmussen et al. 2014a, 2016) and future changes in clouds and precipitation, the main objective of this study is to use novel high-resolution convection-permitting simulations using a pseudo-global warming (PGW) technique (Schär et al. 1996; Sato et al. 2007; Hara et al. 2008; Kawase et al. 2009; Rasmussen et al. 2011, 2014b; Lackmann 2013; Liu et al. 2016; Trapp and Hoogewind 2016) for the RCP 8.5 scenario to estimate the fine-scale processes and physical mechanisms that explain changes in the full spectrum of clouds and precipitating systems across the US in a future climate. The PGW method is best used to address the question, “what will today’s weather look like in

Fig. 1 The WRF US CONUS domain used in the simulations. Topography (m) is indicated in the color shading. The region outlined by the black line represents the US Great Plains (USGP) region used in Figs. 9 and 12. The red dots indicate the locations of the soundings in Figs. 13, 14 and 15 (Corpus Christi, TX; Norman, OK; and Topeka, KS)



a future warmer and moister climate?” In a continental mid-latitude region like the US, the thermodynamic environment plays a large role in determining the occurrence of various types of convective systems, whether it is an isolated convective cell or a large organized mesoscale convective system (MCS). Thus, this study will also examine the thermodynamic environment supporting the convective population in a current and future climate to provide additional information on the physical mechanisms that may govern such changes. By using a set of high-resolution convection-permitting simulations employing the PGW method, the results from this study will contribute to a greater understanding of how fine-scale cloud and mesoscale processes and their thermodynamic environments may vary in a warmer climate.

2 Methodology and experimental design

2.1 High-resolution pseudo global warming regional climate simulations

High-resolution convection-permitting regional climate simulations over the contiguous (CONUS) United States were conducted at the National Center for Atmospheric Research (NCAR) Research Applications Lab (RAL) with the Weather Research and Forecasting (WRF) model V3.4.1 and are used in this study (for more details, see Liu et al.

2016). The model was configured to have 4-km horizontal grid spacing with 1360×1016 grid points in a single domain (Fig. 1) and 51 uneven vertical levels with maximum resolution in the boundary layer. The physical parameterization schemes used in the simulations are the Thompson aerosol-aware microphysics (Thompson and Eidhammer 2014), the Yonsei University (YSU) planetary boundary layer (Hong et al. 2006), the rapid radiative transfer model (RRTMG; Iacono et al. 2008), and the Noah-MP land-surface model (Niu et al. 2011) that was improved for the quality of these simulations (see Liu et al. 2016 for specific modifications to the Noah-MP scheme). Large-scale spectral nudging of temperature, geopotential height and wind was applied in the interior of the domain above the planetary boundary layer to minimize inconsistencies between the model simulation and its forcing data. Scales above 2000 km were nudged, allowing the smaller local and mesoscale features to evolve freely within the constraints imposed by the synoptic pattern. More details on the experimental design can be found in Liu et al. (2016).

One of the primary goals of the convection-permitting high-resolution simulations is to examine water cycle changes over North America under projected climate warming. To achieve this goal, two experiments were conducted using the WRF model framework described above. First, a retrospective or control simulation (CTRL) was conducted for a continuous 13-year period (1 October 2000–2030

September 2013) over the US CONUS domain forced by ERA-Interim reanalysis every 6 h.

The second simulation was a climate sensitivity experiment using the pseudo global warming (PGW) approach, which has been employed in numerous regional climate simulations around the world (Schär et al. 1996; Sato et al. 2007; Hara et al. 2008; Kawase et al. 2009; Rasmussen et al. 2011, 2014b; Lackmann 2013; Prein et al. 2015, 2016, 2017; Liu et al. 2016; Trapp and Hoogewind 2016). This second simulation was conducted for the same continuous 13-year period (1 October 2000–2030 September 2013) forced by ERA-Interim reanalysis plus a climate perturbation derived from a 19-model CMIP5 ensemble monthly mean climate change signal for the RCP8.5 scenario. As described in Liu et al. (2016), the WRF input for the PGW simulation is as follows:

$$\text{WRF}_{\text{INPUT}} = \text{ERA} - \text{Interim} + \Delta\text{CMIP5}_{\text{RCP8.5}} \quad (1)$$

where $\Delta\text{CMIP5}_{\text{RCP8.5}}$ is the 95-year CMIP5 multi-model ensemble-mean monthly change under the RCP8.5 scenario:

$$\Delta\text{CMIP5}_{\text{RCP8.5}} = \text{CMIP5}_{2071-2100} - \text{CMIP5}_{1976-2005} \quad (2)$$

The perturbed fields that were used to generate the WRF input for the PGW simulation include horizontal wind, geopotential, temperature, specific humidity, sea surface temperature, soil temperature, sea level pressure, and sea ice. Across the CONUS domain, temperature changes in the summer and spring in the PGW simulation are approximately +3–6 °C (Liu et al. 2016). More information on the model framework and design of these simulations can be found in Liu et al. (2016).

A limitation of convection-permitting climate simulations is their high demand for computational resources that does not allow for the generation of multi member ensembles to assess uncertainties in climate change projections. The largest uncertainties in these projections are related to atmospheric circulation aspects whereas thermodynamic changes are much more certain (e.g., Bengtsson et al. 2006; Shepherd 2014). In fact, Bengtsson et al. (2006) showed that synoptic wave activity does not show significant changes in a future climate in the ECHAM5 model for the A1B scenario in the winter months. Selecting a single climate model realization as driving data for our future simulation would be highly subjective and might lead non-representative results due to the large intermodel spread between different GCMs (Hawkins and Sutton 2011) and the considerable internal variability on decadal time scales (Deser et al. 2012). The PGW approach avoids the subjective selection of a driving model and simulation period and instead uses 30-year average climate change signals that are representative of a 19-member GCM ensemble under the assumption that the sub-monthly weather patterns will not change significantly in the future climate period. This eliminates decadal variability and

uncertainty introduced by the choice of ensemble member (Deser et al. 2012). Assessing climate change signals with the PGW approach is feasible since the full climate change signal from a GCM-driven regional climate simulation can be decomposed into three additive terms (Kröner et al. 2016): (1) a large-scale thermodynamic effect, (2) lapse-rate effect, and (3) large-scale circulation change. Our study fully considers climate change effects from the first and second term. The third term is not accounted for since systematic changes in the storm tracks are not included, since only sub-synoptic scales are allowed to evolve freely.

For both the CTRL and PGW experiments described above, we will examine the warm season months of May through August for each simulation. Liu et al. (2016) noted the presence of a near-surface warm bias over the US Great Plains during the summer months (JJA) and the bias is greatest in late summer (August–September). A late summer near-surface temperature warm bias is also present in many GCM and regional model simulations (Morcrette et al. 2013). Thus, to ensure that the results from this study are robust and not a result of the late summer warm bias, the analysis is conducted for May–June (MJ) and July–August (JA) separately, since May and June show little to no evidence of a warm bias in the US Great Plains (Liu et al. 2016). In addition, Prein et al. (2017) demonstrate that for these simulations, the frequency of propagating MCSs are well represented in May and June and their characteristics (i.e., speed, size, intensity, and translation) are realistic compared to observations, even in the summer. This provides confidence that this set of simulations is suitable to investigate the effect of climate change on the full convective¹ population.

2.2 Precipitation, atmospheric moisture, and convective population analysis

To assess changes in precipitation in a warmer climate, hourly precipitation output from the WRF simulations is used to calculate the annual average accumulated precipitation for the May–June (MJ) and July–August (JA) periods in the CTRL and PGW simulations. In addition, hourly precipitation is used to calculate the annual mean MJ and JA diurnal cycle of the peak precipitation amount, frequency, and intensity. First, the average climatological precipitation amount for each hour of the day is calculated

¹ Throughout this paper, we use the term “convective population” to refer to the full spectrum of precipitating systems identified by weak through strong radar reflectivity values. Although the nature of the clouds producing a storm’s precipitation may be both convective or stratiform, stratiform precipitation during the warm season is typically either attached to active convection or was previously active convection that decayed into stratiform precipitation.

and the hour with the largest precipitation amount is recorded at each location and is designated the time of peak precipitation. Second, the frequency of hourly precipitation rates that exceed 0.1 mm h^{-1} are summed for each hour of the day at each grid cell and the hour with the highest frequency at each location is designated the time of peak frequency. Finally, the intensity of hourly precipitation is calculated by identifying hourly precipitation rates that exceed 0.1 mm h^{-1} at each grid cell, averaging the precipitation rates for each hour of the day, and then assessing the hour with the highest average precipitation rates at each location, which is designated the time of peak intensity. The hour of peak precipitation is assessed for the CTRL and PGW simulations to investigate changes in the diurnal cycle in a warming climate. In addition to precipitation, changes in atmospheric moisture are calculated by assessing the frequency of occurrence of a relatively high value of column-integrated water vapor (precipitable water; $\geq 50 \text{ mm}$) at each grid point over the 13-year period in each simulation.

One of the primary goals of this study is to assess changes in the convective population in a warming climate over North America. A diagnosis of the convective population requires an investigation of the full spectrum of convection, from weak to extreme deep convection. The methodology used in this study employs composite reflectivity (dBZ), defined as the maximum reflectivity from any level at each grid point, from the CTRL and PGW WRF simulations. Hourly composite reflectivity data from each simulation set is used to calculate the frequency of occurrence in seven reflectivity ranges defined as weak convection (0–10, 10–20 dBZ), moderate convection (20–30, 30–40 dBZ), and strong convection (40–50, 50–60, 60–70 dBZ). The difference (PGW-CTRL) of the frequency of occurrence for each range represents potential future changes in the convective population in the weak to strong convection categories. Finally, the difference between the PGW and CTRL occurrences within each reflectivity range, expressed as a percentage relative to the CTRL population, was calculated using the following formula:

$$\Delta CONV = \frac{(\sum RR_{PGW} - \sum RR_{CTRL})}{\sum RR_{CTRL}} \times 100 \quad (3)$$

where $\Delta CONV$ is the percentage change in the convective population in a future climate, RR is the reflectivity range, and the summation of RR is the total number of times the reflectivity range occurred in each simulation. This metric reveals the change in the PGW convective population relative to the CTRL population and will be used to look at the full CONUS domain and the US Great Plains region in Sect. 4.

2.3 Thermodynamic environments

In the context of the convective population, examining the thermodynamic environments supporting convection is important for understanding potential changes in a warmer climate. For this study, thermodynamic parameters, including convective available potential energy (CAPE; J kg^{-1}) and convective inhibition (CIN; J kg^{-1}), are calculated using hourly output from the CONUS WRF simulations. Both CAPE and CIN are calculated using an average air parcel from the lowest 100 hPa of the atmosphere at each grid point, which is sometimes referred to as Mixed Layer CAPE (MLCAPE). MLCAPE is a measure of the total amount of potential energy available to the mixed layer parcel while being lifted to its level of free convection and is commonly used to assess severe weather potential. CIN is the amount of energy inhibiting convection and can help determine whether a given environment is conducive to explosive deep convection or unfavorable for convection. In an environment with weak inhibition ($\text{CIN} < -50 \text{ J kg}^{-1}$) and high MLCAPE, surface heating can usually break the capping inversion and convective elements are likely to occur, but may not be severe. Environments with moderate inhibition ($-50 \text{ J kg}^{-1} > \text{CIN} > -200 \text{ J kg}^{-1}$) can be overcome with stronger surface heating, synoptic scale lifting, topographic lifting, lifting along a dry line, etc. The presence of moderate CIN allows for CAPE to build up to higher values and with extra lifting or strong surface heating, explosive severe convection can result. However, if the CIN is too strong ($\text{CIN} < -200 \text{ J kg}^{-1}$), the strength of the capping inversion is often too much to overcome and convection is suppressed. As a side note, the CIN ranges described above are typically used to forecast the occurrence of severe deep convection, so the influence of strong CIN is more significant for weaker convective elements in low to moderate MLCAPE environments. This study will look at potential future changes in both MLCAPE and CIN that would provide a different thermodynamic environment for a future convective population.

2.4 Atmospheric sounding analysis

Radiosonde observations from the universal radiosonde observation program (RAOB; <http://www.raob.com/>) are used to evaluate the performance of the WRF runs in simulating free atmospheric conditions at 0 UTC. For each sounding location shown in Tables 1 and 2, vertical profiles of WRF data are created by selecting the temperature, dewpoint temperature, and wind speed at the closest grid cell to the sounding site. All observed and modeled 0 UTC soundings are interpolated to common sigma coordinate levels that range from 1 to 0.05 in 0.01 intervals and the median soundings are calculated. Finally, MLCAPE, CIN and 0–6 km wind shear are calculated for each sounding

Table 1 List of sounding parameters calculated at various stations across the central US

Station	Location	Mean MLCAPE (CTRL)	Mean MLCAPE (PGW)	CTRL mean CIN	PGW mean CIN
72250	Brownsville, TX	<i>1292/1543</i>	<i>2104/2368</i>	<i>-201/-103</i>	<i>-250/-155</i>
72251	Corpus Christi, TX	<i>1121/1211</i>	<i>1904/2023</i>	<i>-218/-147</i>	<i>-265/-196</i>
72261	Del Rio, TX	<i>1011/521</i>	<i>1603/1007</i>	<i>-166/-71</i>	<i>-220/-102</i>
72240	Lake Charles, LA	<i>779/1278</i>	<i>1349/2023</i>	<i>-131/-84</i>	<i>-181/-131</i>
72233	Slidell, LA	<i>727/1001</i>	<i>1183/1698</i>	<i>-82/-64</i>	<i>-128/-94</i>
72235	Jackson, MS	<i>473/705</i>	<i>755/1158</i>	<i>-75/-57</i>	<i>-107/-85</i>
72248	Shreveport, LA	<i>545/588</i>	<i>913/977</i>	<i>-96/-48</i>	<i>-142/-78</i>
72249	Fort Worth, TX	<i>674/429</i>	<i>1082/769</i>	<i>-130/-55</i>	<i>-184/-90</i>
72265	Midland, TX	<i>592/440</i>	<i>1000/806</i>	<i>-101/-52</i>	<i>-153/-85</i>
72364	El Paso, TX	<i>546/543</i>	<i>974/1130</i>	<i>-31/-37</i>	<i>-52/-54</i>
72365	Albuquerque, NM	<i>849/833</i>	<i>1409/1649</i>	<i>-22/-37</i>	<i>-39/-54</i>
72363	Amarillo, TX	<i>500/464</i>	<i>882/860</i>	<i>-81/-59</i>	<i>-123/-91</i>
72355	Fort Sill, TX	<i>632/414</i>	<i>1056/695</i>	<i>-121/-65</i>	<i>-172/-101</i>
72357	Norman, OK	<i>611/416</i>	<i>1002/669</i>	<i>-119/-66</i>	<i>-163/-96</i>
72340	Little Rock, AR	<i>463/512</i>	<i>737/812</i>	<i>-74/-49</i>	<i>-123/-82</i>
72327	Nashville, TN	<i>345/474</i>	<i>560/794</i>	<i>-51/-49</i>	<i>-83/-81</i>
72440	Springfield, MO	<i>455/438</i>	<i>757/611</i>	<i>-72/-59</i>	<i>-118/-90</i>
72456	Topeka, KS	<i>466/441</i>	<i>780/556</i>	<i>-88/-73</i>	<i>-129/-115</i>
72451	Dodge City, KS	<i>431/473</i>	<i>733/770</i>	<i>-85/-74</i>	<i>-134/-108</i>
72469	Denver, CO	<i>619/902</i>	<i>1113/1908</i>	<i>-32/-46</i>	<i>-53/-59</i>
72562	North Platte, NE	<i>343/573</i>	<i>565/837</i>	<i>-62/-78</i>	<i>-104/-110</i>
72558	Omaha Valley, NE	<i>369/447</i>	<i>626/559</i>	<i>-67/-76</i>	<i>-117/-120</i>
72649	Chanhassen, MN	<i>194/302</i>	<i>324/375</i>	<i>-33/-55</i>	<i>-56/-92</i>

All parameters are derived from the 0 UTC soundings at each station. The values in each category are listed for May–June (MJ) and July–August (JA) in the following arrangement: MJ/JA. Italicized values in the table indicate that the distribution mean values between the CTRL and PGW simulations are significantly different according to the non-parametric Mann–Whitney U test at a 0.05 level

profile using the lowest 100-hPa parcel method described in Sect. 2.3.

To facilitate the analysis of how an idealized sounding would change under varying temperature conditions, the classic Weisman and Klemp (1982) sounding, which is appropriate for an environment supporting convective weather, is used in Sect. 5.3. For this analysis, the air temperature is shifted by a constant value (± 5 °C) and dewpoint temperatures are adjusted to conserve relative humidity. MLCAPE and CIN are then calculated for the original and shifted profiles to determine the change in thermodynamic parameters under changing temperature conditions.

3 Precipitation and atmospheric moisture

To obtain an understanding of how precipitation may vary with climate change, monthly averaged precipitation accumulation values are calculated for the CTRL and PGW simulations (Fig. 2). In MJ, moderate precipitation is widespread east of the Rockies in the US and Mexico and throughout

most of Canada (Fig. 2a, b). The difference (PGW-CTRL) of precipitation in MJ (Fig. 2c) shows moderate increases in precipitation across Canada (~ 10 – 30 mm increase), a complex pattern of precipitation changes over the US Great Plains, substantial precipitation increases in Texas and the Gulf of Mexico, and decreases in precipitation over the Atlantic and the Caribbean. Moving to the warm season, CTRL precipitation in JA is less widespread across the US Great Plains, which is related to a model dry bias of up to 50%, and is more abundant over the Sierra Madre Mountains in Mexico, southeastern US, Gulf of Mexico, and Atlantic Ocean (Fig. 2d). The difference of precipitation in JA (Fig. 2f) shows large decreases over the US Great Plains (~ 10 – 30 mm), moderate increases over the mountainous regions of Mexico and the US, large increases in the northern Gulf of Mexico and southern US, and decreases over the southern Gulf of Mexico and the Caribbean.

The diurnal cycle of precipitation is very important, because certain types of convective systems tend to maximize at different times of the day. Afternoon convection responding to diurnal heating of the land surface usually

Table 2 Differences (PGW-CTRL) in the sounding parameters calculated at various stations across the central US

Station	Location	Mean MLCAPE difference (MJ)	Mean MLCAPE diff. (JA)	Mean CIN diff. (MJ)	Mean CIN diff. (JA)
72250	Brownsville, TX	812	825	-49	-52
72251	Corpus Christi, TX	783	812	-47	-49
72261	Del Rio, TX	592	486	-54	-31
72240	Lake Charles, LA	570	745	-50	-47
72233	Slidell, LA	456	697	-46	-30
72235	Jackson, MS	282	453	-32	-28
72248	Shreveport, LA	368	389	-46	-30
72249	Fort Worth, TX	408	340	-54	-35
72265	Midland, TX	408	366	-52	-33
72364	El Paso, TX	428	587	-21	-17
72365	Albuquerque, NM	560	816	-17	-17
72363	Amarillo, TX	382	396	-42	-32
72355	Fort Sill, TX	424	281	-51	-36
72357	Norman, OK	391	253	-44	-30
72340	Little Rock, AR	274	300	-49	-33
72327	Nashville, TN	215	320	-32	-32
72440	Springfield, MO	302	173	-46	-31
72456	Topeka, KS	314	115	-41	-42
72451	Dodge City, KS	302	297	-49	-34
72469	Denver, CO	494	1006	-21	-13
72562	North Platte, NE	222	264	-42	-32
72558	Omaha Valley, NE	257	112	-50	-44
72649	Chanhassen, MN	130	73	-23	-37

All parameters are derived from the 0 UTC soundings at each station. Italicized values in the table indicate that the distribution mean values between the CTRL and PGW simulations are significantly different according to the non-parametric Mann–Whitney U test at a 0.05 level

maximizes in the early to mid- afternoon, while larger and more organized mesoscale convective systems (MCSs) have a nocturnal maximum. GCMs do not accurately reproduce the diurnal cycle of precipitation over land and thus detailed mesoscale and cloud processes are not adequately represented in coarse-resolution climate modeling (Allen and Ingram 2002). Trapp et al. (2010) showed that using a convection-permitting regional climate simulation can produce the correct diurnal cycle of precipitation. One motivation for using a convection-permitting horizontal resolution in this study is to more accurately represent the physical processes of the convective lifecycle, including the initiation, upscale growth, and decay of propagating MCSs (Trapp et al. 2010; Liu et al. 2016; Prein et al. 2016, 2017). Prein et al. (2017) uses a Lagrangian feature-tracking algorithm to identify and track MCSs in the same set of simulations used in the current study. Comparisons with radar and gauge based precipitation measurements show that the model is able to reproduce the main characteristics of MCSs, such as their size, translation speed, and maximum rainfall rates, within observational uncertainties in most regions of the US. In addition, their results highlight that MCSs are also

realistically simulated in regions that show significant frequency biases, such as the central US.

Another way to diagnose if a particular model framework can reproduce the full lifecycle of convection is to examine the diurnal cycle of precipitation. Figures 3 and 4 present a comparison of the diurnal cycle of the peak precipitation amount, frequency, and intensity over the US from Stage IV radar-derived precipitation observations and the CTRL and PGW experiments in MJ and JA, respectively. In addition, statistical significance using the Mann–Whitney U test and a significance level of 0.05, represented as white dots on Figs. 3b, f, j and 4b, f, j, shows if the annual peak times in the amount, frequency, and intensity of rainfall are statistically different between the CTRL simulation and Stage-IV observations (i.e., if the differences are larger than the inter-annual variability). In a similar manner, the white dots on Figs. 3c, g, k and 4c, g, k show statistically significant differences between the PGW and CTRL simulations. Overall, the almost random distribution of the white dots in Figs. 3 and 4 across the continental US indicate that there are no statistically significant biases in the CTRL vs. Stage-IV observations, except in regions where the Stage-IV data is

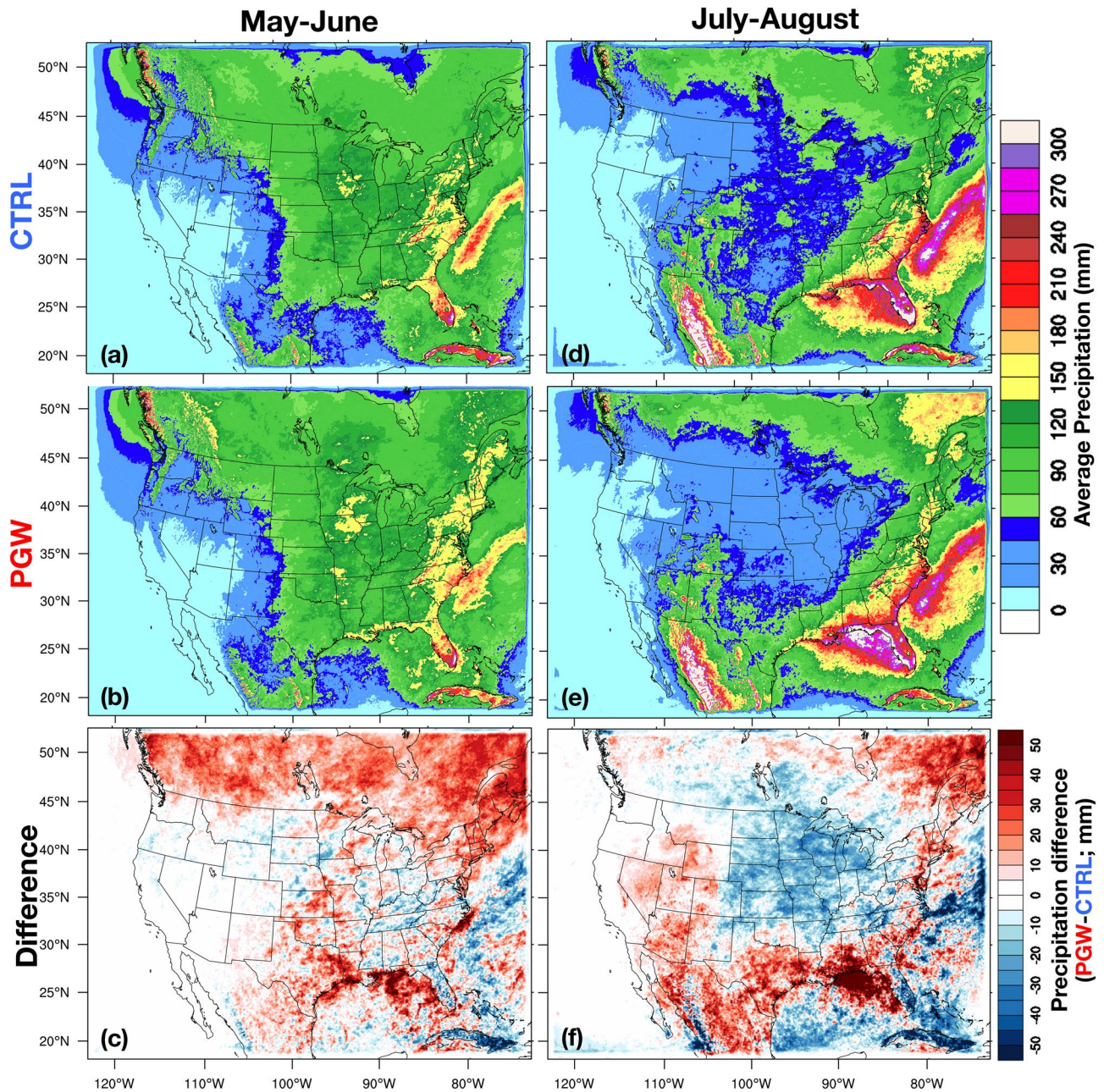


Fig. 2 Average accumulated precipitation (mm) in May–June (left column) and July–August (right column) for the entire 13-year CTRL (top row) and PGW (middle row) simulations. The bottom row presents the difference (PGW-CTRL) of the average accumulated precipitation

well known to be of poor quality because of the lack of radar observations (e.g., over oceans and Canada). In addition, the random distribution of white dots in Figs. 3c, g, k and 4c, g, k indicate that the differences in the PGW simulation are not statistically significant and may be attributed to interannual variability.

In MJ, the spatial pattern of the peak diurnal precipitation amount from the CTRL model simulation is consistent with the observations, with a nocturnal maximum east of the Rockies (Fig. 3a, b). The peak intensity of precipitation

shows a clear progression from 22–24 UTC (late afternoon in local time) over the central Rockies to 10–14 UTC (early morning in local time) over the central US, likely associated with propagating nocturnal MCSs. A similar diurnal cycle of precipitation frequency is seen in the CTRL simulation in MJ compared to the observations, although the observations show later peak precipitation frequency times than the CTRL simulation during the nocturnal hours (Fig. 3e, f). The precipitation intensity observations in MJ (Fig. 3i, j) exhibit a somewhat similar pattern to the frequency observations

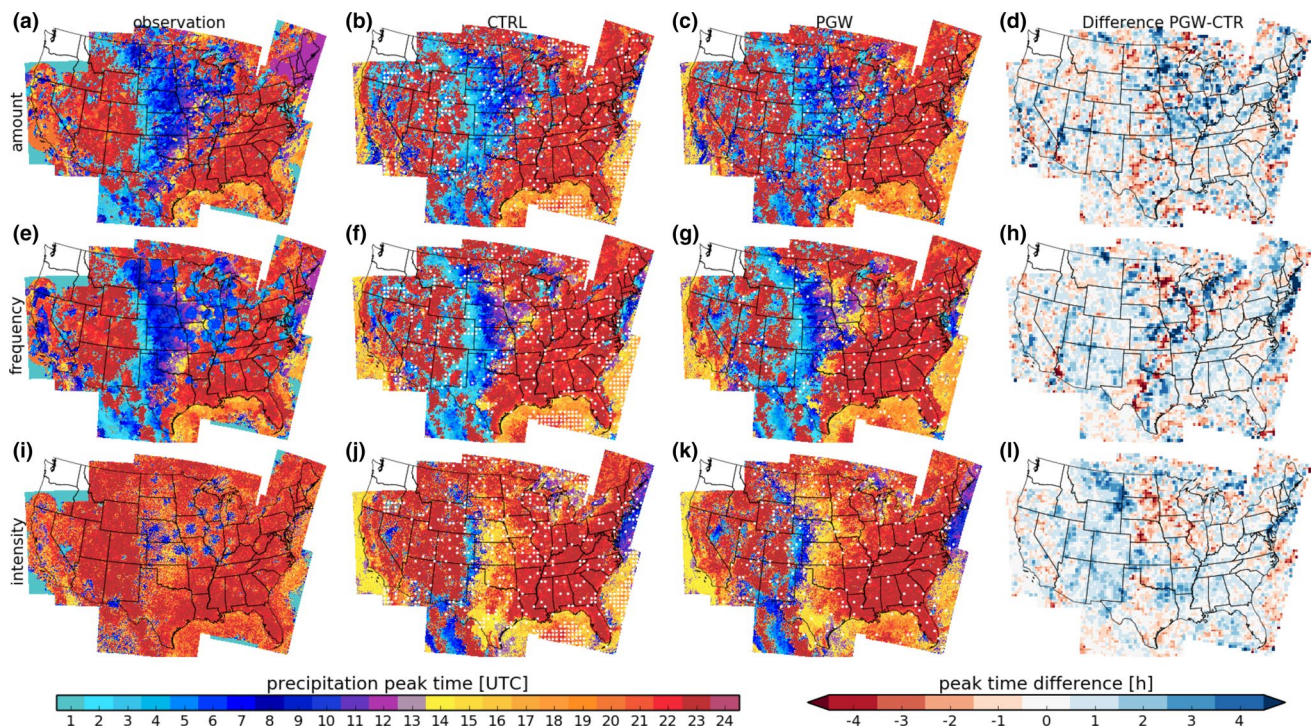


Fig. 3 The maximum hour of the diurnal cycle of precipitation over the US in May–June is shown from (1) Stage-IV observations in the first column, (2) the CTRL simulation in the second column, (3) the PGW simulations in the third column, and (4) the difference of PGW-CTRL in the right column. For each dataset or model simulation, the time of peak precipitation (UTC) is shown in terms of precipitation amount (top row), precipitation frequency (middle row), and precipi-

tation intensity (bottom row) for comparison. The white dots in **b, f, j** indicate statistically significant differences (using the Mann–Whitney U test and a significance level of 0.05) between the Stage-IV observations and the CTRL precipitation metrics. The white dots in **c, g, k** indicate statistically significant differences using the same method as above, but between the PGW and CTRL precipitation metrics

(Fig. 3e, f), with a narrower extent east of the Rockies foothills. Dai et al. (1999) found that diurnal variations in precipitation intensity are not as large as precipitation amount or frequency over the US and are less spatially coherent even in summer. The round radar disks visible in Fig. 3i indicate that perhaps the Stage-IV dataset may not capture the full spatial variability of the precipitation intensity across the US, but the similarity to the CTRL simulation (Fig. 3j) is apparent. From Oklahoma through the Dakotas, the peak time for precipitation intensity is around 12–14 UTC (early morning in local time), again indicating the importance of nocturnal MCS precipitation in this region. MCSs are known to contribute between 30–70% of warm season precipitation in the US (Fritsch et al. 1986; Carbone and Tuttle 2008), thus accurately representing the MCS lifecycle is critical for assessing potential future changes in convection and the water cycle over the US.

Future changes in the diurnal cycle of peak precipitation amount, frequency, and intensity are not very large in the PGW simulations in MJ (Fig. 3c, d, g, h, k, l). However, the late evening to nocturnal precipitation signals appear to expand slightly to the north in the PGW simulations. This is especially notable in the peak diurnal frequency and

intensity panels (Fig. 3f–h, j–l) that show an expansion of the 10–14 UTC peak frequency and intensity to the northeast of the CTRL panels (Fig. 3f, j). Given that a future climate will be warmer, the expansion of propagating convection to the north and to the east is somewhat expected and populations in the northern US and southern Canada downstream of the Rockies may see increased organized convection in MJ.

During the late summer (JA), a similar diurnal cycle of precipitation is seen in the observations with an eastward progression of precipitation amount, frequency, and intensity from the Rockies to the Midwest (Fig. 4a, d). Compared to MJ in Fig. 3, the signature of propagating organized convection lasting into the early morning is more robust and extends farther east in JA. The CTRL simulation peak precipitation amounts are different from the observations, especially after ~8 UTC in the central Great Plains. The peak diurnal precipitation frequency (Fig. 4f) has a similar pattern as the amount while differences to the observations are largest for the timing of precipitation intensities (Fig. 4j). This indicates that the JA CTRL simulation likely represented propagating convection, but did not have enough MCSs given the lower amounts in the central Great Plains.

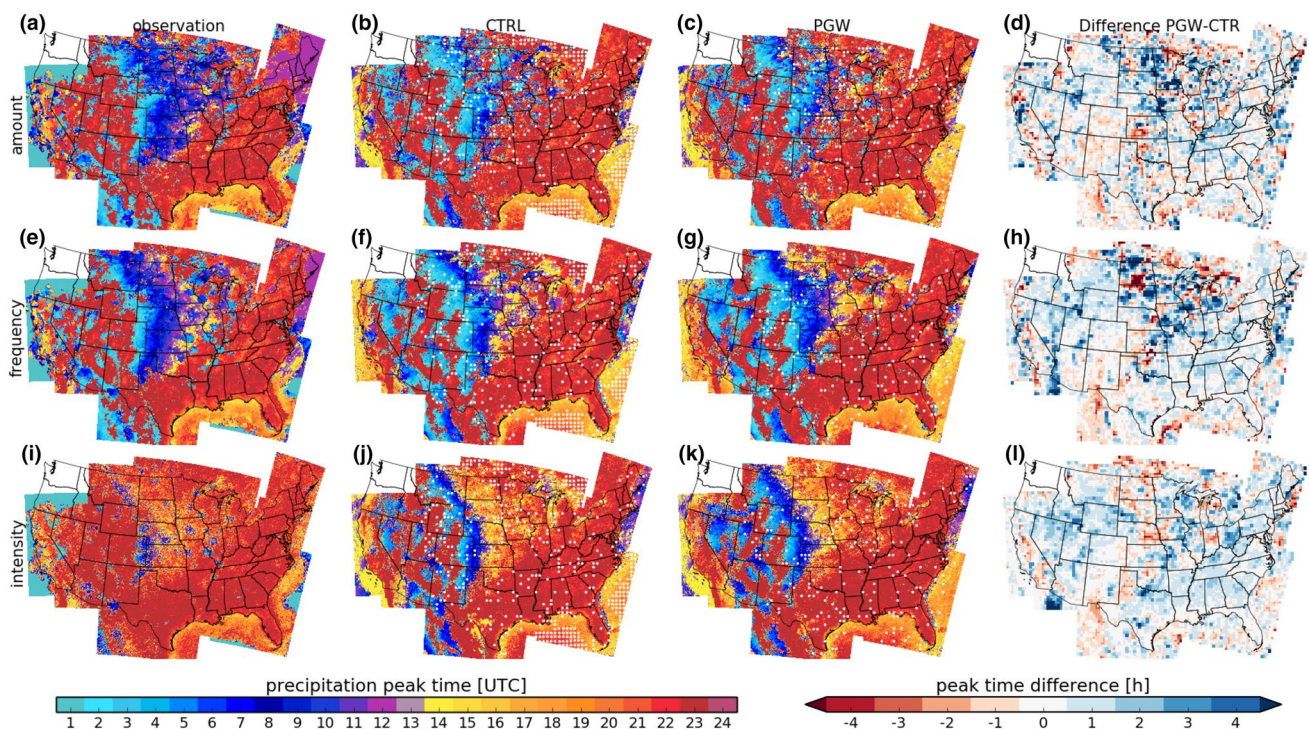


Fig. 4 As in Fig. 3, but for the months of July–August

A recent study by Prein et al. (2017) using the same CONUS WRF simulations also showed that the CTRL run had too few propagating mesoscale convective systems in the late summer compared to observations. They also showed that the size and intensity of convective systems closely matched the observations, providing confidence that when the model does produce a propagating convective system, it is a fairly realistic representation of actual MCSs, which is difficult for most coarse resolution climate models to reproduce. Thus, although the convective systems are too few in the PGW simulation, their lifecycle and propagation characteristics closely resemble the observations (Prein et al. 2017). The results for the peak diurnal cycle in the PGW simulation show a similar pattern as the CTRL runs, with an expansion of nighttime peaks to the north and east (Fig. 4d, h, l) as was similarly shown for MJ in Fig. 3. As discussed for Fig. 3, the warmer temperatures of the PGW runs are the likely reason for this shift to the north and an analog can be seen in the precipitation diurnal cycle observations for MJ compared to JA (Figs. 3a, e, i, 4a, e, i).

To investigate how atmospheric moisture content will change in a warmer climate, frequency changes in an extreme value of the column-integrated water vapor in the atmosphere (precipitable water; mm) are investigated using a threshold of 50 mm as described in Sect. 2.2. Figure 5 shows the monthly average number of precipitable water occurrences ≥ 50 mm for the CTRL and PGW simulations

in MJ and JA. Results from the CTRL simulation for MJ show relatively few instances of high precipitable water (Fig. 5a). The PGW simulation has about double the number of occurrences of high precipitable water, with regions in the Caribbean having ~ 3 – 4 times more occurrences than the CTRL simulation (Fig. 5b). A northward expansion of high precipitable water frequency is seen downstream of the Rockies, likely associated with the low-level jet bringing moister air into the continental US. A similar result is found for JA, with the PGW simulation having ~ 2 – 3 times more high precipitable water occurrences than the CTRL simulation (Fig. 5c, d). The northward expansion of high precipitable water is more pronounced in JA compared to MJ, supporting the hypothesis that the low-level jet brings more moisture from the Gulf of Mexico into the continental US during the warm season. More available moisture in the eastern US downstream of the Rockies will likely affect the distribution and character of convection that will be examined in the next section.

4 Convective population changes in a future climate

In a future climate, the scientific consensus is that extreme storms will become more extreme (Trenberth et al. 2003; Romps et al. 2014; Ban et al. 2015; Prein et al. 2016). While

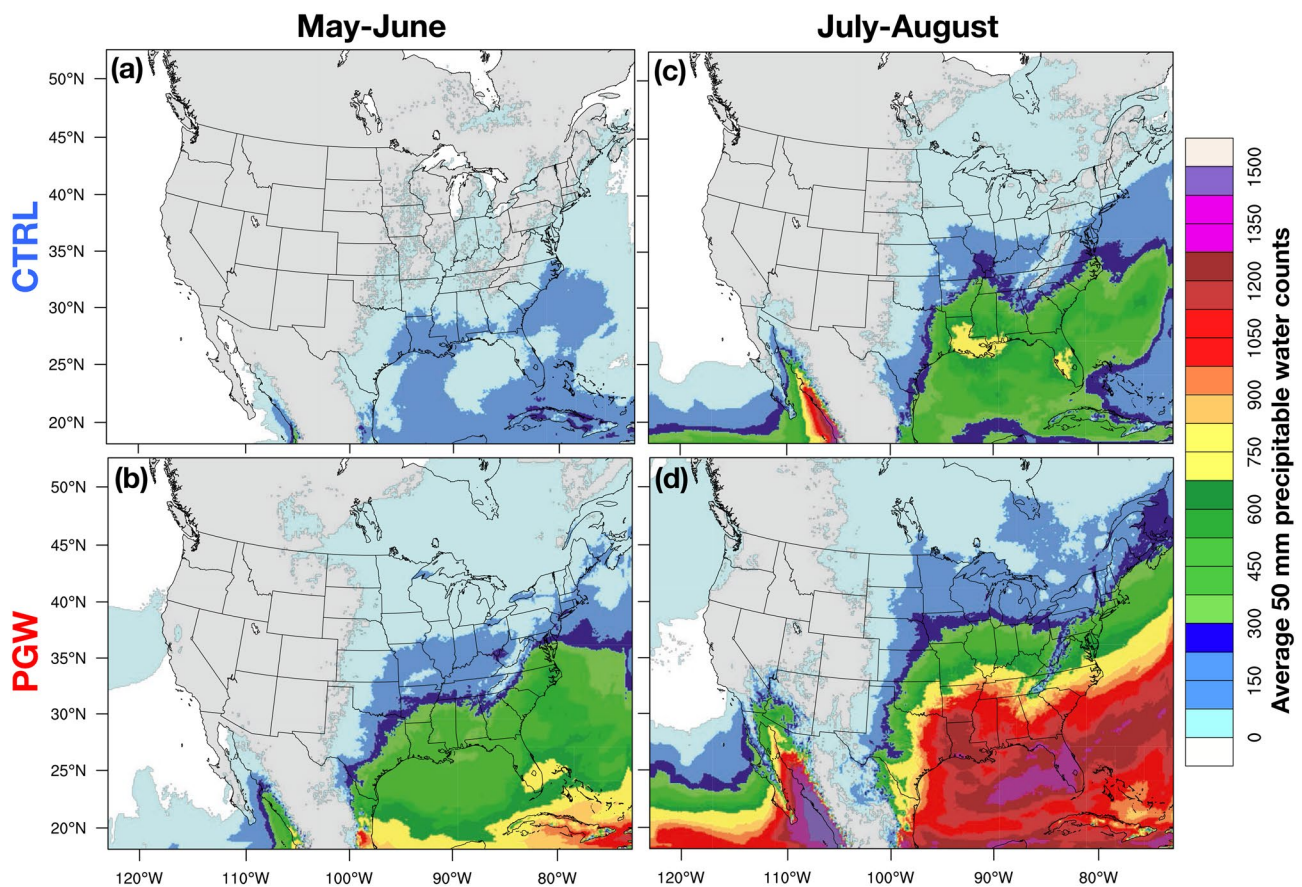


Fig. 5 Frequency of 50 mm precipitable water occurrences over the CONUS domain in all 13-years of the simulations are shown by season (May–June and July–August) and by simulation type (CTRL and

PGW). The color shading represents the average number of occurrences per year exceeding the 50 mm precipitable water threshold value as described in Sect. 2.2

this has been a robust result across various modeling platforms with coarse to fine horizontal resolution, an understanding of the behavior of the full spectrum of the convective population is important for assessing changes in the diurnal and seasonal cycles of convective systems during the warm season in the US. The current study uses a methodology to examine weak to strong precipitating systems in the convection-permitting CONUS WRF simulations. As described in Sect. 2.2, seven reflectivity ranges are used for the analysis of the convection in the CTRL and PGW simulations. Composite reflectivity is used to capture the three-dimensional structure of the convection by choosing the largest value of reflectivity in the column above any given grid point, thus the method does not miss high values of reflectivity. To provide context for the analysis of the convective population in the section below, Fig. 6 shows average reflectivity values for the 13-year simulations in MJ and JA for the CTRL and PGW simulations. Higher reflectivities are located in Canada in MJ relative to the US (Fig. 6a), most likely due to the synoptic activity over the northern region of the domain in the late spring, which is consistent with Prein

et al. (2017). General decreases in composite average reflectivity over the US in the PGW simulation (Fig. 6b) indicates a shift in the convective population that will be examined in the analysis of the seven reflectivity ranges below.

The results for the reflectivity analysis are presented in Figs. 6 and 7 for MJ and JA, respectively. The convective population in MJ, represented as differences (PGW-CTRL) in the frequency of occurrence within each reflectivity range, is presented in Fig. 7. A widespread decrease in occurrence of the weak reflectivity echoes (0–10; 10–20 dBZ) is seen across North America, indicating that fewer weak precipitating systems will be present in a warmer climate in MJ (Fig. 7a, b). This decrease even extends over oceans and is most notable over the intermountain west, Pacific Northwest, and northeast regions of the US. The moderate reflectivity ranges (20–30, 30–40 dBZ) show robust increases in convection across continental Canada and moderate increases in the southwest US and over the Rockies in Colorado and Arizona (Fig. 7c, d). Large regions of decreasing moderate convection are still seen across the US east of the Rockies extending into the Atlantic Ocean and along the Pacific

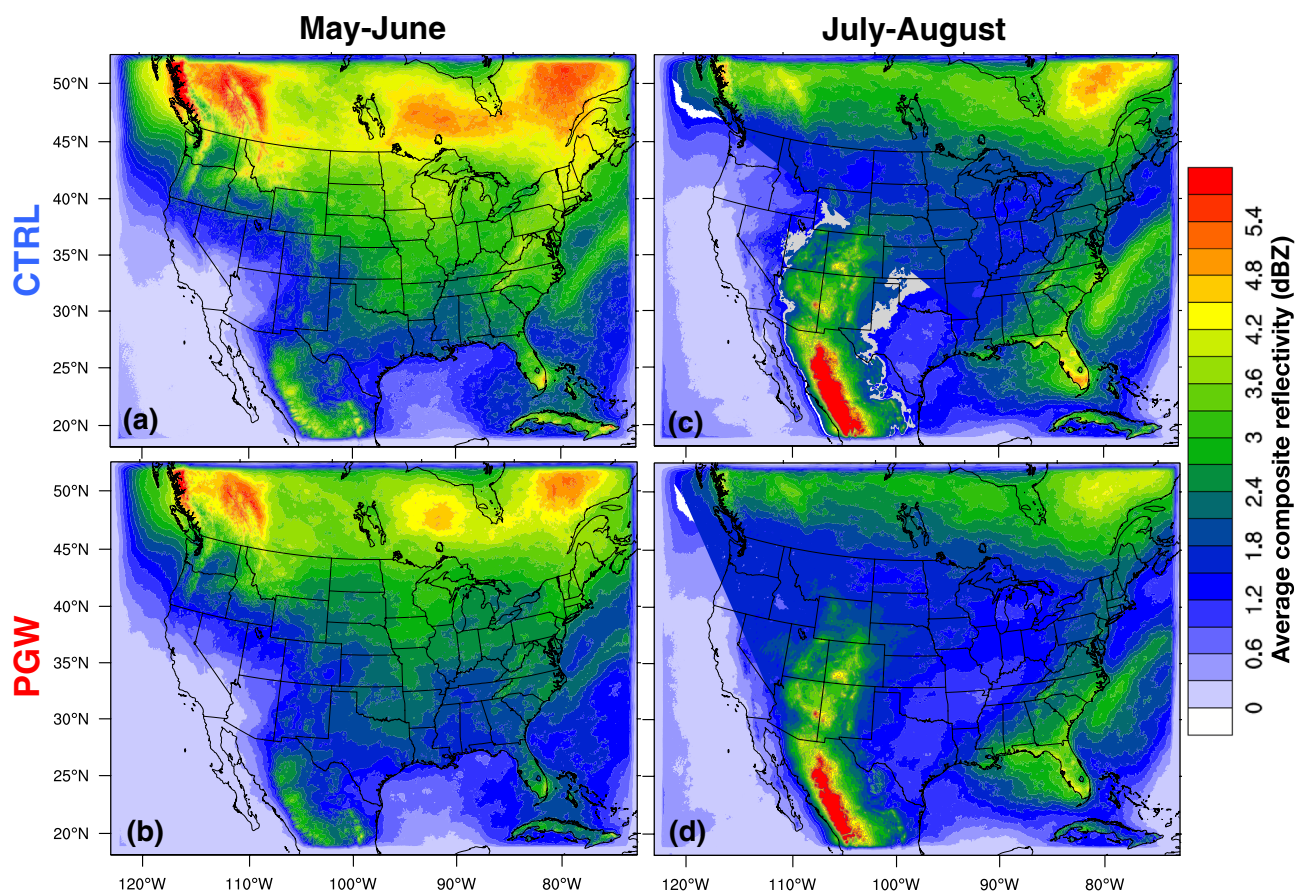


Fig. 6 Average composite reflectivity over the CONUS domain in all 13-years of the simulations are shown by season (May–June and July–August) and by simulation type (CTRL and PGW)

Northwest coastal mountain ranges. Increasing moderate convection in the 30–40 dBZ range is observed along the Gulf Coast (Fig. 7d) that is also seen in the strong reflectivity ranges (40–50, 50–60 dBZ; Fig. 7e, f). The robust increase in strong reflectivity ranges is notable across Canada, and more moderate increases can be seen across the continental US, with small regions of decreases in the eastern US. The strongest reflectivity range (50–60 dBZ) shows increases across most of North America (Fig. 7f), consistent with the scientific consensus that extreme convection will become more extreme in a warmer climate.

Moving to the late summer, Fig. 8 shows the six reflectivity range difference results for JA. In the weak reflectivity ranges (0–10, 10–20 dBZ), a strong departure from the MJ patterns is seen in the western US and Mexico (Fig. 8a, b). In fact, increases are seen in these regions in all six reflectivity ranges in Fig. 8. An increase in the entire convective population in the western US indicates that storms of all intensities may become more frequent in a future climate in this region, and is supported by increases in monthly average accumulated precipitation by ~10–20 mm in the PGW simulations in JA in these regions (Fig. 2f). Increases in

the occurrence of ≥ 50 mm precipitable water amounts also increase in the PGW simulation in the southwestern US, indicating strengthening precipitating systems in JA associated with the southwestern monsoon. While a detailed study on the specific mechanisms increasing precipitation, moisture and convection in the western US is beyond the scope of this study, further research on the future changes in the convective population will be conducted given the large focus on water resources and management in the western US.

As Figs. 7 and 8 show, the patterns of changes in the convective population are not as simple as the “wet gets wetter, dry gets drier” argument (Held and Soden 2006; Liu and Allan 2013), since many complex synoptic, mesoscale and cloud processes are important for determining what type of convective system occurs in any particular environment. A summary of the convective population changes is presented in Fig. 9, showing the $\Delta CONV$ parameter (Eq. 3) for each reflectivity range in MJ and JA. In general, the lower reflectivity ranges occur less frequently in a future climate and the higher reflectivity ranges are more frequent in both the full CONUS domain and the US Great Plains (black box in Fig. 1). Across the

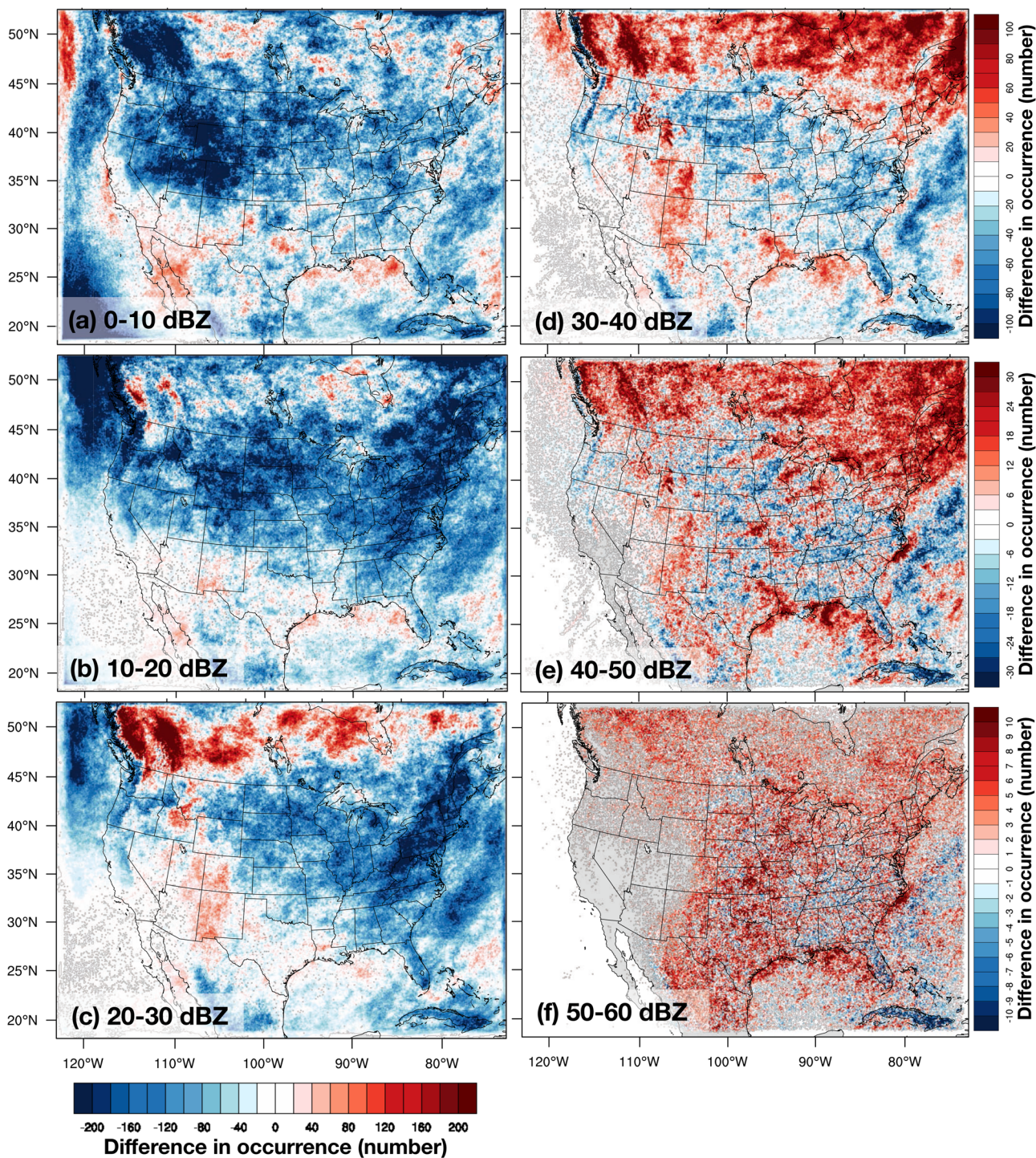


Fig. 7 Difference maps (PGW-CTRL) of the occurrence of six reflectivity thresholds at each grid point in May–June, defined in Sect. 2.2: **a** 0–10 dBZ, **b** 10–20 dBZ, **c** 20–30 dBZ, **d** 30–40 dBZ, **e**

40–50 dBZ, and f 50–60 dBZ. Note that the color bar for panels (a–c) are the same and the color bars for panels (d–f) are presented to the right of each figure

entire CONUS domain, the MJ and JA changes are relatively similar, with the exception of the near zero change in the 60–70 dBZ range in MJ, providing confidence that this is a robust signal even with the warm bias in

the central US. The simulated changes in the US Great Plains might be affected by the simulated warm and dry bias in this region (Figs. 8, 9b), but the overall signal of the change is similar between MJ and JA, with JA showing

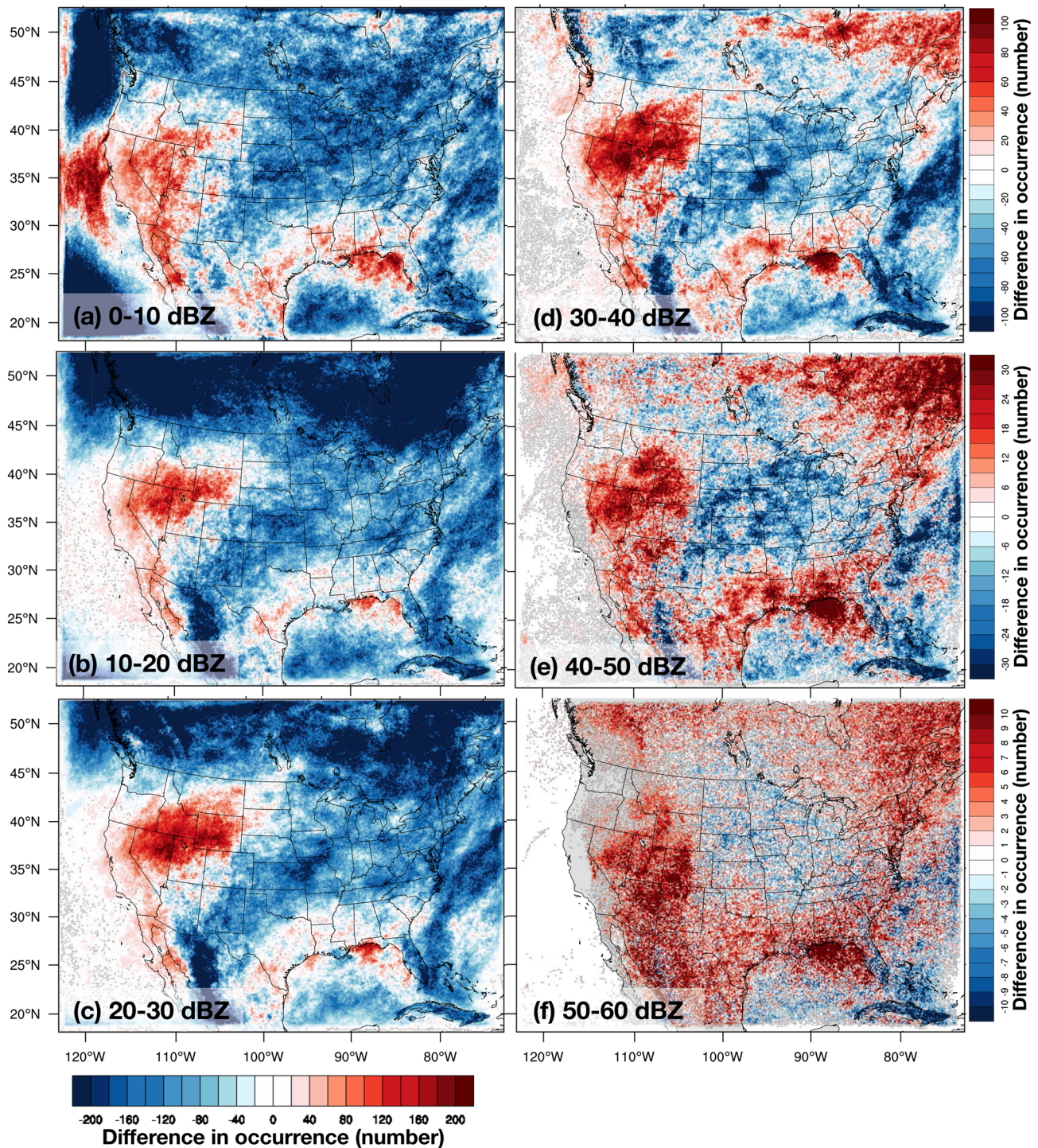


Fig. 8 As in Fig. 7, but for the months of July–August

a more pronounced decrease in the convective population from 0 to 60 dBZ (Fig. 9). Thus, the decreasing frequency of weaker precipitating systems and increases in strong precipitating systems are a robust result. To understand

why these changes in the convective population may occur in a warmer climate, an analysis of the thermodynamic environments supporting the convective population is presented in Sect. 5.

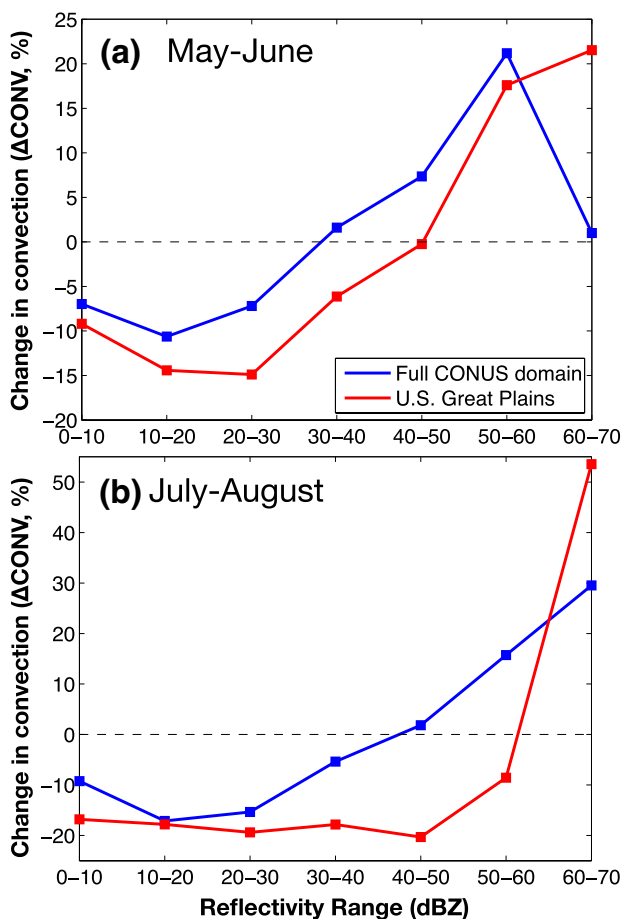


Fig. 9 Summary of the total change in occurrence of each reflectivity range in the full CONUS domain and in the US Great Plains (USGP) region, indicated by the red box in Fig. 1. The total number of occurrences in each range are summed in each domain and $\Delta CONV$ is calculated according to Eq. 3. This metric indicates the change in the PGW convective population relative to the CTRL population, expressed as a percentage and shown as a function of the reflectivity range (dBZ) for **a** May–June and **b** July–August

5 Thermodynamic environment in a future climate

The thermodynamic environment supporting convection can determine whether a convective system will initiate, the intensity of the storm once initiated, storm characteristics, and much more. Many thermodynamic indices have been developed in the operational and research severe weather community to predict the occurrence of severe storms and to understand why different types of convective systems occur (Doswell 1985; Craven et al. 2002). Results from this study show that the convective population is expected to have fewer weak to moderate storms and more strong convection in a warmer climate (Figs. 7, 8, 9; Sect. 4). In the context of the high-resolution regional climate simulations used in this study, the convective elements were allowed to develop

naturally in the larger-scale synoptic and thermodynamic environments provided by the CTRL and PGW-perturbed simulations. Given that the development of convective systems was directly influenced by differences in the thermodynamic environments in the CTRL vs. PGW-perturbed simulations, this section will examine changes in the bulk thermodynamic conditions to provide insights into the physical mechanisms responsible for the corresponding changes in the convective population. As was described in Sect. 2.3 above, mixed-layer convective available potential energy (MLCAPE; $J kg^{-1}$) and CIN ($J kg^{-1}$) are used to look at overall changes in the thermodynamic environment in the following sections.

5.1 Bulk thermodynamic environmental changes

Figure 10 presents the monthly average MLCAPE and CIN from the CTRL and PGW simulations and their differences in MJ. In the CTRL simulation, moderate values of MLCAPE and CIN are located east of the Rocky Mountains in the active convective region of the US (Fig. 10a, d). The effect of the low-level jet bringing warm and moist air into the US continent from the Gulf of Mexico is apparent in these figures and has been well documented in the current climate (Carlson et al. 1983; Geerts et al. 2016). A comparison of the meridional moisture flux in the region of the low-level jet and Gulf of Mexico between the ERA-Interim reanalysis and CTRL simulation (not shown) shows that the model is consistent with the moisture and flow characteristics in this region. Immediately east of the Rockies, moderately strong values of CIN are typically generated by dry air flowing over the Rocky Mountains, diurnal heating from the Mexican Plateau, and other sources of midlevel subsidence in the region (Carlson et al. 1983). Moderate CAPE and CIN allow for the gradual build-up of convective energy and is typically released through enhanced lifting along a dryline or a synoptic short wave trough (Carlson et al. 1983). Thus, the region of moderate MLCAPE and CIN downstream of the Rockies provides a favorable environment for moderate to strong convection in the late spring and early summer months in the central Great Plains.

Changes in the thermodynamic environment in the PGW-perturbed simulation are presented in Fig. 10b, c, e, f. Both MLCAPE and CIN increase in magnitude east of the Rocky Mountains, with a clear preference for increases directly east of the mountains. This result indicates that there is more energy available for convection and more energy inhibiting convection, which is complementary to the results from Sect. 5 showing that the occurrence of weaker reflectivity echoes decreases and the occurrence of higher reflectivity echoes increases in a warmer climate. Even with more MLCAPE in the thermodynamic environment, corresponding increases in CIN results in a shift of the convective

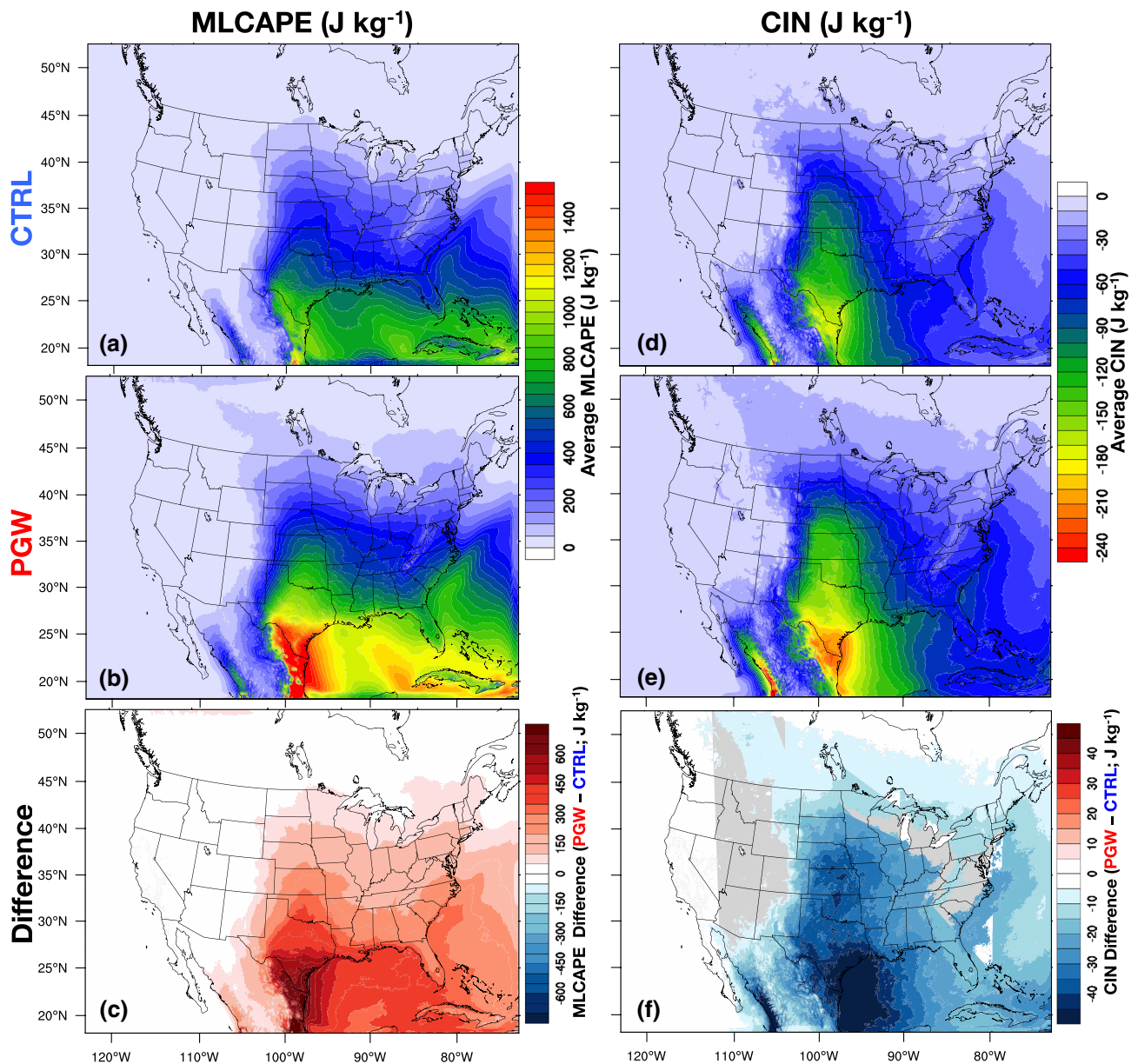


Fig. 10 Average thermodynamic parameters for May–June are shown for the CTRL (top row) and PGW (middle row) simulations and their differences (bottom row). Mixed-layer convective available potential

energy (MLCAPE; J kg^{-1}) is presented in the first column and convective inhibition (CIN; J kg^{-1}) is presented in the second column

population spectrum because weak to moderate convection may be suppressed, which modifies the spatial and temporal occurrence of precipitating systems across the US.

As was previously shown, the air above the Gulf of Mexico is expected to have significantly more moisture in the future compared to the current climate (Fig. 5), thus the low-level jet will likely provide greater moisture flux convergence over the central US downstream of the Rockies. The penetration of relatively high values of precipitable water (≥ 50 mm) into the US continent was shown in Fig. 5 and likely contributes to the tongue of stronger CAPE values

(between 50 and 500 J kg^{-1}) immediately downstream of the Rockies in the central Great Plains (Fig. 10b, c). A corresponding increase in the magnitude of CIN is observed downstream of the Rockies as well (Fig. 10e, f). Over the Gulf of Mexico, higher moisture also results in more MLCAPE over that region, but increasing CIN results in decreases in weaker reflectivity echoes typically associated with maritime precipitating systems (Fig. 7a–c).

The thermodynamic environment for the current and future simulations in JA is presented in Fig. 11. Similar to Fig. 10a, d, the MLCAPE and CIN in the US in JA is

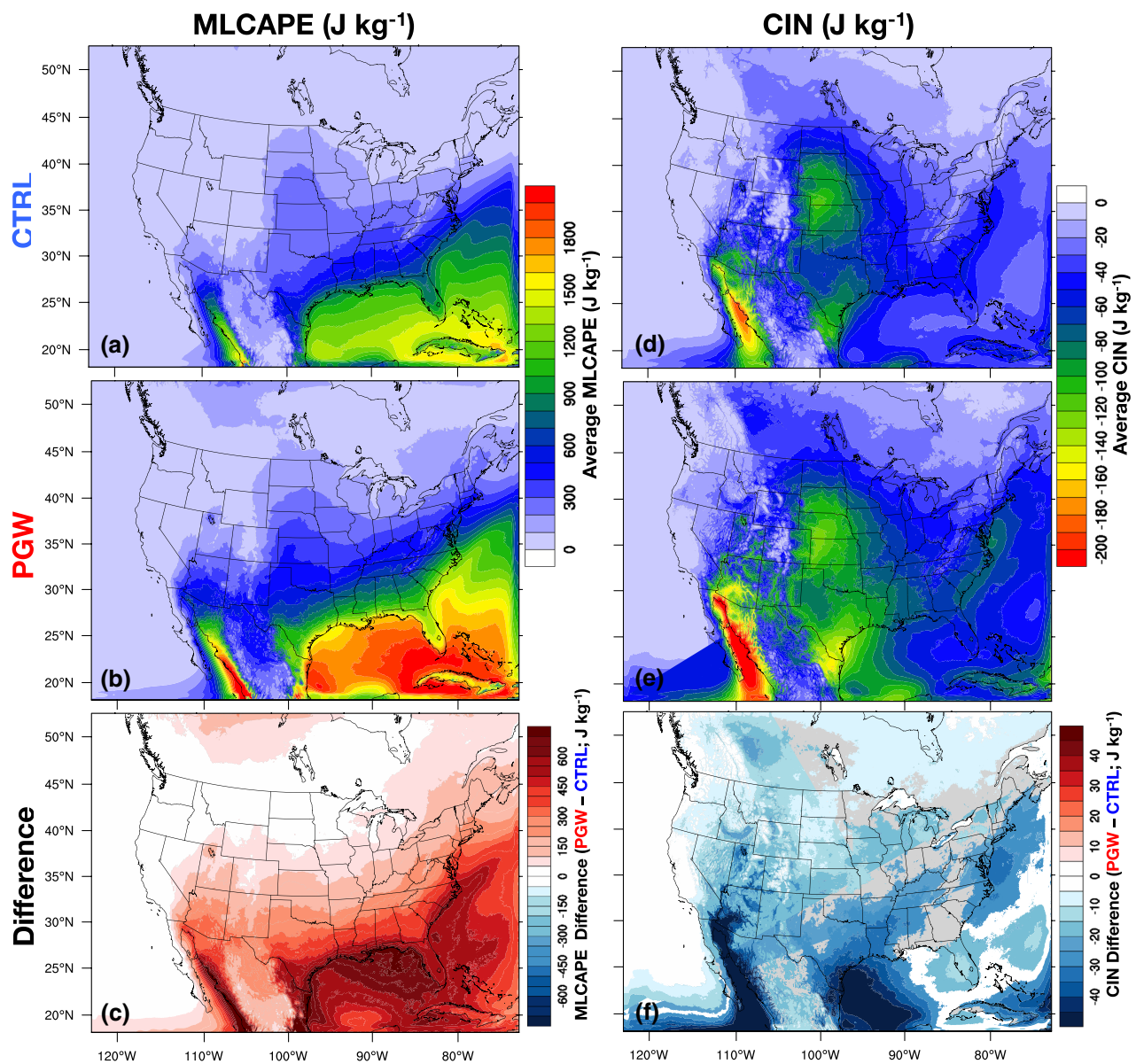


Fig. 11 As in Fig. 10, but for the months of July–August

mostly concentrated east of the Rocky Mountains, with generally weaker MLCAPE and CIN shifted to the north and extending into Canada (Fig. 11a, d). During the summer, the low-level jet reaches much farther north compared to the spring and brings warm and moist air into the US and Canada east of the Rockies (Geerts et al. 2016). Frequent intense convective systems occur in a broad geographical region from Texas through the Dakotas and east during the later summer, as was shown by the geographical variability in observed MCSs during the Plains Elevated Convection at Night (PECAN) field campaign in summer 2015 (Geerts et al. 2016).

Similar to the results from Fig. 10, both MLCAPE and CIN increase in magnitude in the PGW simulation in late summer (Fig. 11b, c, e, f). However, although the increases directly downstream of the Rockies in JA are not as apparent as in MJ, the influence of the low-level jet advecting very moist air from the Gulf of Mexico into the continental US downstream of the Rockies is clear. In addition, large increases in magnitude in both MLCAPE and CIN over the Gulf of Mexico leads to decreases in the occurrence of reflectivity echoes between 0 and 50 dBZ since lifting mechanisms to break through the stronger cap are not typically present over the ocean. An exception to this pattern is the

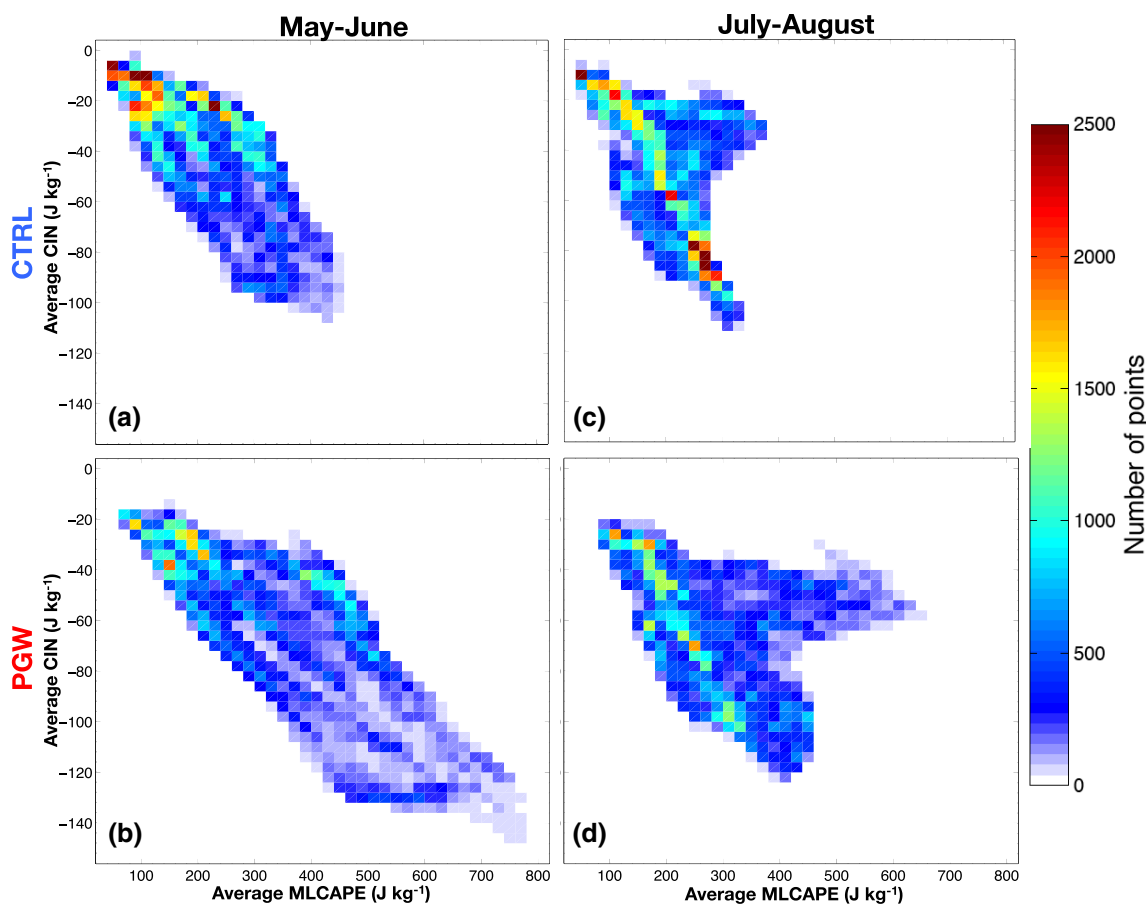


Fig. 12 Two-dimensional histogram of average MLCAPE vs. CIN in **a, b** May–June and **c, d** July–August for the entire 13-year simulation datasets. Histograms for the CTRL simulation are presented in

the top row and the PGW simulation are presented in the bottom row. The color shading represents the number of times each MLCAPE and CIN combination occurred

increase in convective activity across all reflectivity ranges along the Gulf Coast from Louisiana through Florida that may be related to increased tropical convection or a potential enhancement in land-sea breezes, but is beyond the scope of the present study and will be examined in future research.

Focusing on the US Great Plains region, Fig. 12 shows a comparison of the thermodynamic environments supporting convection in the CTRL and PGW simulations for both MJ and JA. In each panel of Fig. 12, the thermodynamic environment is represented by the relationship between MLCAPE and CIN and how frequently the environment occurs. In the CTRL simulation in MJ (Fig. 12a), low values of CIN and MLCAPE are the most frequent, with an extension to approximately -100 J kg^{-1} of CIN and 400 J kg^{-1} of MLCAPE representing a relatively narrow range. In the CTRL simulation in JA (Fig. 12c), a higher frequency of environments with moderate CIN and MLCAPE are observed compared to MJ (Fig. 12a). In addition, a protrusion to higher MLCAPE values in the environmental characteristics is seen between -20 and -50 J kg^{-1} of CIN and represents a different mode of the thermodynamic

environment during JA associated with a different spectrum of convective systems that have higher values of MLCAPE but weaker CIN to overcome.

In a future climate, the thermodynamic environments supporting convection represent a broader distribution of MLCAPE and CIN values in both MJ and JA (Fig. 12b, d). Compared to the CTRL simulation in MJ, the PGW distribution shows a significant expansion to almost double the MLCAPE values and 1.5 times the CIN values in Fig. 12b. This expansion represents a modulation in the thermodynamic environments supporting convection in the US Great Plains and helps explain the shift in the convective population shown in Figs. 7 and 9. While the environment can support more vigorous convective storms, the capping inversion is stronger and requires more energy to break through. Thus, the convective population changes in MJ shown in Figs. 7 and 9 are consistent with these simultaneous changes in the thermodynamic environment, with fewer weak to moderate storms and more intense storms. The thermodynamic environment in the PGW simulation in JA shows a similar, but less pronounced expansion to higher CAPE and CIN values

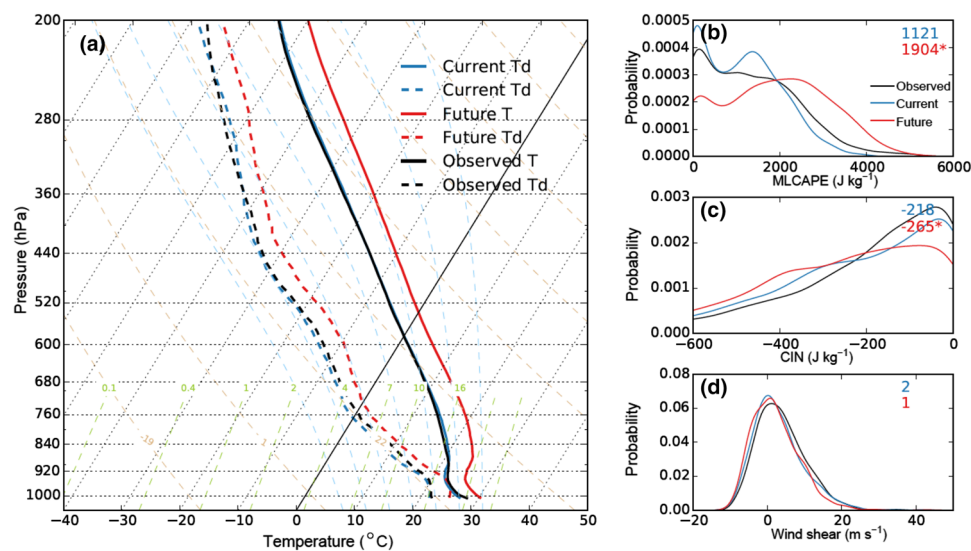


Fig. 13 **a** Median atmospheric thermodynamic sounding profiles from Corpus Christi, Texas at 0 UTC in MJ, plotted on a skew-T diagram. The solid lines indicate the temperature (T) profiles for the observations (black), CTRL simulation (blue), and PGW simulation (red). The dashed lines indicate the dewpoint temperature (Td) profiles for the observations (black), CTRL simulation (blue), and PGW simulation (red). **b** Probability density function (PDF) of the range of

MLCAPE (J kg^{-1}) values in the observations (black), CTRL simulation (blue), and PGW simulation (red). **c** As in (b), but for the range of CIN (J kg^{-1}) values. **d** As in (b), but for the range in 0–6 km wind shear (m s^{-1}). Numbers in the upper right of (b–d) show the mean values of the PDFs. An asterisk symbol shows that the PGW mean value is significantly different from the CTRL mean values according to the Mann–Whitney U test at the 0.05 level

(Fig. 12d). However, the most notable difference in the PGW JA distribution (Fig. 12d) is the lateral expansion of the aforementioned bulge in moderate CIN values to higher MLCAPE values, indicating a shift in the thermodynamic environment supporting convection in the late summer.

These results are consistent with state-of-the-art climate model simulations that suggest future increases in hazardous convective weather due to an increase in CAPE (Trapp et al. 2007, 2009; Diffenbaugh et al. 2013; Brooks 2013; Lackmann 2013; Gensini and Mote 2014; Trapp and Hoogewind 2016). Other studies have demonstrated that CAPE is expected to increase in a warming climate using an idealized Radiative Convective Equilibrium (RCE) perspective appropriate for tropical environments (Muller et al. 2011; Igel et al. 2013; Singh and O’Gorman 2013; Romps 2016; and many others). However, the results of this study suggest that the amount of energy inhibiting convection (CIN) is critical to understanding changes in the convective population in the US and surrounding maritime environments. Increases in the amount of both MLCAPE and CIN over the Gulf of Mexico also result in a decrease in the weak to moderate precipitating systems south of the coastal region (Figs. 5a–c, 7a–c), indicating a strong response in tropical maritime environments as well. Thus, a more comprehensive understanding of the changes in the convective population in a future climate likely requires a full diagnosis of changes in the thermodynamic environment in all climate regimes around the world.

5.2 Specific changes in thermodynamic profiles in a future climate

A typical method to examine the thermodynamic conditions of the atmosphere is to use atmospheric sounding data collected from rawinsondes. The examination of bulk thermodynamic metrics in Sect. 5.1 demonstrated the geographic variability of future changes in the thermodynamic environment across the US and how those changes resulted in a shifting convective population. In this section, sounding observations at various sites across the US are compared to both the CTRL and PGW simulations to provide greater confidence in both the model representation of thermodynamic environments and future changes in those environments. The methodology for the sounding analysis is described in Sect. 2.4 and all sounding comparisons are at 0 UTC to capture the environment most relevant to convective storms across the US.

Atmospheric sounding observations from three stations (Corpus Christi, TX; Norman, OK; and Topeka, KS) are compared to model-derived thermodynamic profiles from the closest grid point to these stations from the CTRL and PGW simulations in Figs. 13, 14 and 15. The median temperature and dewpoint observations are notably similar to the profiles derived from the CTRL simulation at all three stations (Figs. 13, 14, 15), providing confidence in the ability of the CTRL simulation to capture atmospheric thermodynamic properties. As Liu et al. (2016) showed, the addition

Fig. 14 As in Fig. 13, but for the Norman, Oklahoma station

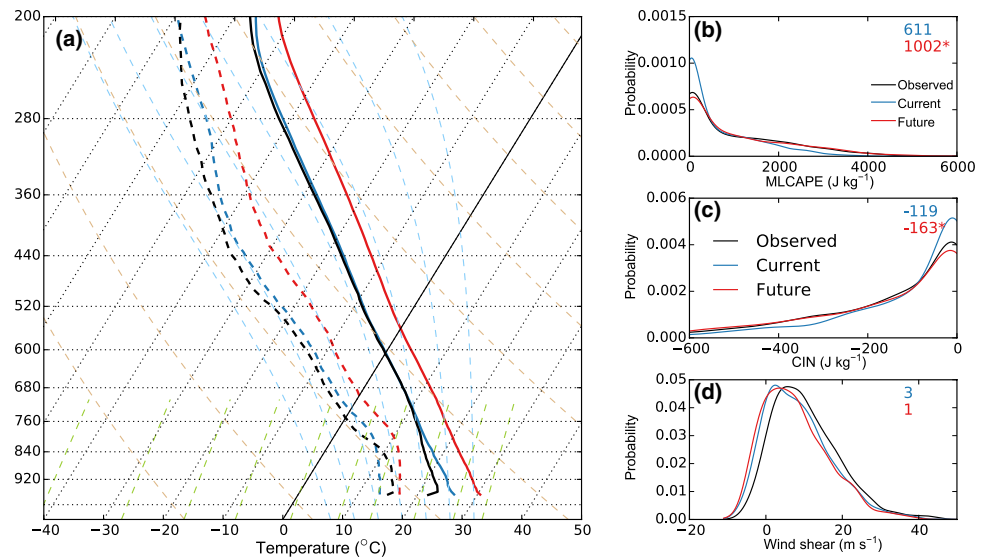
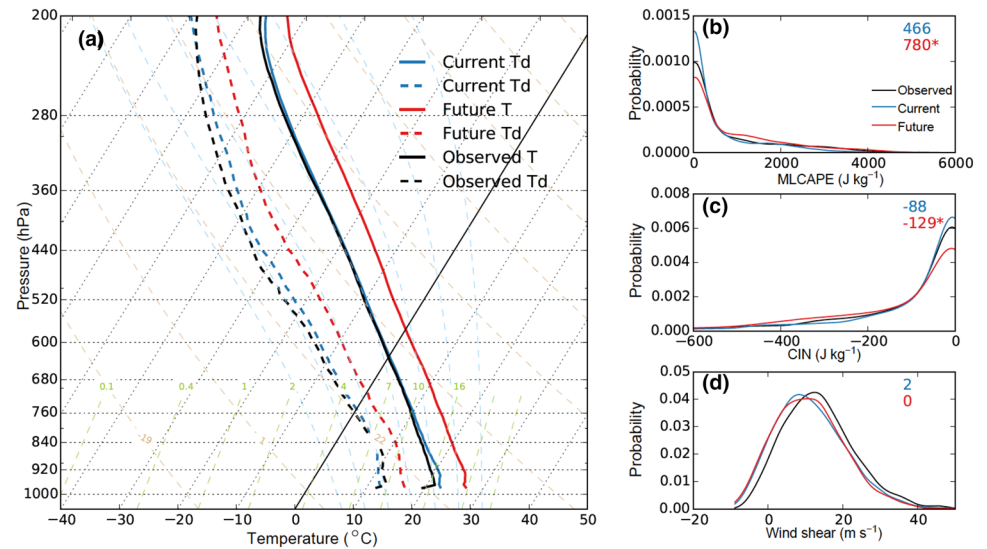


Fig. 15 As in Fig. 13, but for the Topeka, Kansas station



of the PGW perturbations resulted in a general warming and increase in moisture throughout the troposphere. A result of the warmer and moister troposphere is the higher frequency of large MLCAPE values, as demonstrated by the probability density function figures showing the range of MLCAPE in all derived profiles in the 13-year dataset (Figs. 13b, 14b, 15b). Mean MLCAPE values increase in a warmer climate by an average of 783 J kg^{-1} at Corpus Christi, TX, 391 J kg^{-1} at Norman, OK, and 314 J kg^{-1} at Topeka, KS with all of these differences being statistically significant according to the non-parametric Mann–Whitney U test at the 0.05 level. While the increase in MLCAPE is most notable at the Corpus Christi location (Fig. 13b), all 23 stations analyzed in the central US showed increasing mean MLCAPE in the PGW simulation (Tables 1, 2), which supports the results from Figs. 10, 11 and 12 and Sect. 5.1.

A similar analysis was conducted for CIN in each observational and model-derived sounding profile and the results are presented in Figs. 13c, 14c, and 15c for the three stations and for all stations in Tables 1 and 2. Overall, probability density functions show that in the PGW simulation, CIN values are expected to increase in magnitude and provide a stronger capping inversion or more energy inhibiting convection. Mean CIN values increased in magnitude by 47 J kg^{-1} at Corpus Christi, TX, 44 J kg^{-1} at Norman, OK, and 41 J kg^{-1} at Topeka, KS with all of these differences being statistically significant according to the non-parametric Mann–Whitney U test at the 0.05 level (Figs. 13c, 14c, 15c). Similar to the increases in MLCAPE at all stations, CIN also increased in magnitude at all stations examined in this analysis (Tables 1, 2). The sounding locations represent different environment conditions since Norman, OK and

Topeka, KS are located at a continental region, while Corpus Christi, TX is located at a coastal region. Regardless of the region, these stations show the same sign of the changes in MLCAPE and CIN. Thus, these results are consistent with the analysis from Figs. 10, 11 and 12 and Sect. 5.1 and demonstrate a robust response in the thermodynamic environment supporting convection in a warmer and moister climate.

In convective storm development and organization, the amount of vertical wind shear is important in determining the mode of convection as shown by Rotunno et al. (1988) and many other studies. Thus, an analysis of the magnitude of the 0–6 km vertical wind shear in each sounding profile was calculated and the probability density functions are presented in Figs. 13d, 14d, and 15d for the three stations. The wind shear at all three stations decreases in the PGW simulation and thus is likely not responsible for the differences in the convective population presented in Figs. 7, 8 and 9. However, the use of spectral nudging at the large scales in these simulations limits full shear changes from being realized, as noted in Trapp et al. (2007). While a detailed investigation of the three-dimensional structure of the precipitating systems is beyond the scope of this study, future research on this topic would provide more information on the three-dimensional characteristics of storms in a changing climate.

5.3 Idealized thermodynamic response in a future climate

From the results presented in Sects. 5.1 and 5.2, the thermodynamic environment in a future climate will provide more energy available for convection and more energy inhibiting convection. The fact that all stations showed statistically significant increases in magnitude in these parameters in the PGW simulation (Table 2) is particularly notable, especially given the complex response of precipitation, convective storm frequency, and many other phenomena to a changing climate (Prein et al. 2015, 2016; Romps et al. 2014). Given the robust response in the thermodynamic environment to a warmer and moister climate, a question arises about the fundamental behavior of MLCAPE and CIN parameters in a cooler vs. warmer climate state. In the context of convective storm dynamics and thermodynamics, the atmospheric sounding profile from Weisman and Klemp (1982), hereafter referred to as WK, is a canonical and standard profile that has been used for decades to test the response of convection to wind shear and many other processes important for convective dynamics (Weisman and Klemp 1982; Rotunno et al. 1988). As described in Sect. 2.4, this study uses the WK sounding and modifies the temperature profile (keeping relative humidity constant) to represent idealized atmospheric conditions for ± 5 °C. Using this approach, the fundamental behavior of both MLCAPE and CIN will be examined for

varying environments and the results will provide a greater understanding of how the thermodynamic environments supporting convection vary with changes in temperature.

The results from the idealized experiment are presented in Fig. 16a, with example profiles from -5 °C and $+5$ °C included with the original WK sounding profile. When temperature is decreased by 5 °C, both the MLCAPE and CIN decrease in magnitude compared to the original profile (MLCAPE and CIN for the WK profile are shaded in red and blue colors, respectively). In contrast, when the temperature is increased by 5 °C, both the MLCAPE and CIN increase in magnitude, echoing the results from the bulk and atmospheric sounding thermodynamic analysis from Sect. 5.1 and 5.2. Given the strong dependence between temperature and the saturation vapor pressure of the atmosphere from the Clausius–Clapeyron equation, the fundamental behavior of both MLCAPE and CIN in a warmer climate is perhaps not a surprising result. This is especially true because both MLCAPE and CIN are calculated using the virtual temperature, which takes atmospheric moisture into account. Thus, if more atmospheric moisture is present in the atmosphere, the parcel will contain more buoyancy than a similar atmosphere with less moisture as is shown graphically in Fig. 16a, b. Similarly, a warmer and moister environment results in a greater magnitude of CIN (Fig. 16c). This relationship holds true for every degree of warming and cooling as demonstrated by the MLCAPE and CIN values in Fig. 16b, c. The slope of the MLCAPE curve is steeper than the CIN curve, indicating the profound role of temperature in generating atmospheric buoyancy and convective energy (Fig. 16b, c). However, as was described in Sect. 2.3, if the CIN is too strong, convection may be inhibited if a lifting mechanism is not present. In a warmer climate, if a significant lifting mechanism is present, the severity of the convection will likely be greater than in the current climate, given that more energy will be available for convection. This result is consistent with other studies showing extreme convective weather events increasing in frequency and intensity in a future climate (Prein et al. 2015, 2016; Ban et al. 2015; Romps et al. 2014).

Results from Lucarini et al. (2010) suggest that entropy production and the degree of irreversibility of the earth system are linearly proportional to the logarithm of CO₂ concentrations. In other words, they propose that the climate system becomes less efficient, more irreversible, and features higher entropy in a warmer climate. From a thermodynamic perspective, higher entropy in the thermodynamic profile for the warmest temperature profile considered in the idealized thermodynamic analysis (Fig. 16) is apparent given the steep slope of the moist adiabatic lines that ultimately determine the amount of MLCAPE in the profile. Since entropy is conserved in a reversible adiabatic process, increases in the irreversibility of the earth system also results in an increase

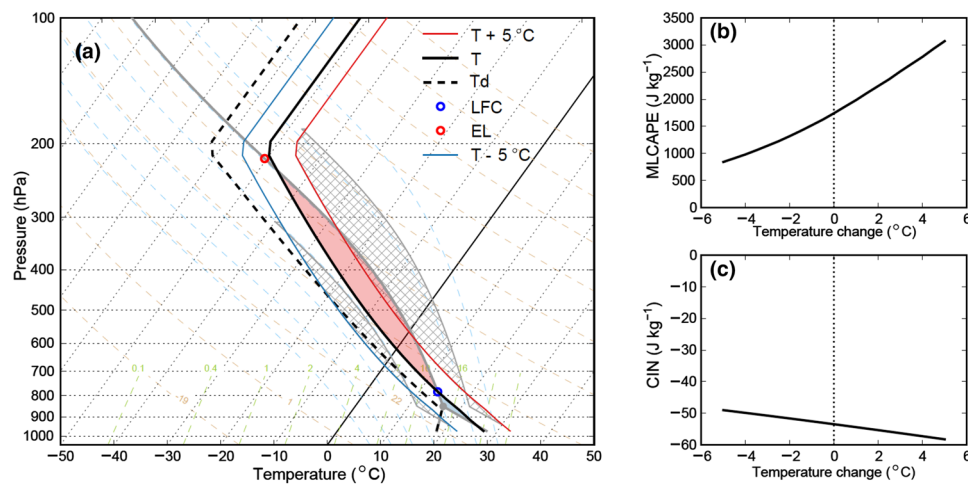


Fig. 16 Idealized thermodynamic analysis using the Weisman and Klemm (1982) sounding profile. **a** The original Weisman and Klemm (1982) sounding profile is shown in black lines (solid-temperature; dashed-dewpoint temperature). MLCAPE and CIN are shown in the red and blue shading, respectively. The level of free convection (LFC) elevated level (EL) are shown in blue and red circles, respectively. The atmospheric temperature was changed by ± 5 °C to test the range in thermodynamic responses with a warmer vs. cooler climate.

The $+5$ °C temperature profile is shown in the solid red line and the -5 °C profile is shown in the solid blue line. The dewpoint temperature profile is shifted by keeping the relative humidity constant. For each of these profiles, the MLCAPE and CIN are shown in light gray hatching. A summary of the **b** MLCAPE and **c** CIN changes with the ± 5 °C temperature variations show a robust relationship to changing temperatures

in entropy (Lucarini et al. 2010). Given that potential temperature is a meteorologist's entropy (Bohren and Albrecht 1998), increased MLCAPE and CIN in the warmest climate ($+5$ °C) are a result from the increasing irreversible processes that span a larger range of potential temperatures (dry adiabatic lines) than cooler temperatures (Fig. 16a). Lucarini et al. (2010) also show that changes in latent heat fluxes are the dominant ingredients for this change, demonstrating the critical importance of representing clouds and precipitation correctly in future climate simulations.

The fundamental relationship between important thermodynamic parameters that are critical to understanding changes in the convective population in a future climate is revealed. Even in the absence of variations in synoptic and mesoscale conditions, a warmer climate will provide greater energy available for convection and also greater energy inhibiting convection. This seesaw effect is critical for understanding potential changes in the convective population across the US and beyond. It explains why the high-resolution convection-permitting simulations show a decrease in weak to moderate precipitating systems and an increase in strong to extreme precipitating systems. The latter result agrees with prior research on this topic, that we can expect more extreme storms and more intense precipitation rates in a warmer climate (Prein et al. 2016). However, when considering convection in general, the detailed thermodynamic conditions are critical to understanding the type and intensity of convection that results. In addition, since the changes of CIN in the idealized profiles are modest relative

to the PGW simulation (Figs. 10, 11, 16), the importance of complex interactions with the Earth system, including land-atmosphere interactions that can influence the thermodynamic environment supporting convection should be explored in future research.

By considering both MLCAPE and CIN in this study, we have shown that it is likely that enhanced CIN in a future climate both suppresses weak to moderate convection across the US, and also provides an environment where convective energy can build to extreme levels and result in more frequent violent severe convection compared to the current climate. Although the relationship between increased MLCAPE and CIN is especially important for mid-latitude continental convective storms, as has also been shown in a previous study looking at extreme tornadic cases using the PGW method (Trapp and Hoogewind 2016), these parameters also appear to explain decreases in weak to moderate convection and increases in strong convection over the Gulf of Mexico, which is predominantly characterized by maritime and tropical convection. The uniform increases in temperature and humidity throughout the troposphere provide a conceptual framework to gain understanding of how such changes will impact the thermodynamic environment of future convection. Studies have shown that upper tropospheric temperatures might increase more in a warmer climate leading to a stabilization of the atmosphere (Liu et al. 2016; Kröner et al. 2016). This would limit the increase in MLCAPE but have no significant effect on CIN. In addition, expected decreases in near surface relative humidity over

land areas (Seager et al. 2007) might affect MLCAPE and CIN. Thus, the interplay between MLCAPE and CIN may be important for many regions of the Earth where convective processes are present and should be considered in future convection-resolving studies on climate change.

6 Conclusions

Two novel high-resolution convection-permitting regional climate simulations are used to investigate changes in the convective population and thermodynamic environments in a future climate and were conducted as follows: (1) 13-year continuous retrospective control simulation forced by ERA-Interim reanalysis every 6 h, and (2) 13-year continuous PGW simulation forced by ERA-Interim reanalysis plus a 19 CMIP5 model monthly mean climate perturbation every 6 h. By comparing these two simulations, this study examines changes in precipitation, the convective population, and the thermodynamic environment supporting convection in the US in a future climate.

Analysis of the diurnal cycle of precipitation in the CTRL simulation in MJ and JA compared to observations showed that the CTRL simulation diurnal precipitation amount, intensity, and frequency is closer to observations than would be possible with a GCM, including a nocturnal peak in precipitation east of the Rockies with an eastward propagating diurnal signal. This similarity indicates that propagating and organized convection is well represented in the CTRL simulation (see also Prein et al. 2017), which is challenging for coarse resolution climate models to represent well. The PGW simulation showed a similar diurnal cycle of precipitation to the CTRL simulation, but with a slight north- and eastward expansion of nocturnal precipitation likely from warmer temperatures providing an environment supporting convection in the northern US and southern Canada east of the Rockies. Given that most GCMs do not have a nocturnal maximum in precipitation over the central US and MCSs are known to contribute ~30–70% of the warm season precipitation, accurately representing organized and propagating systems in climate simulations is critical to a greater understanding of a changing convective population and precipitation in a future climate.

In addition, the frequency of extreme values of high precipitable water (≥ 50 mm) will increase at least twofold over much of the US east of the Rockies, the Gulf of Mexico, and Atlantic Ocean. A northward expansion of high precipitable water occurrences east of the Rockies is particularly notable from the analysis, supporting the expansion of the diurnal cycle of precipitation to the north noted previously. This northward expansion likely results from enhanced moisture flux convergence from the low-level jet bringing warmer

and moister air into the interior of the continental US east of the Rockies.

To investigate changes in the convective population, composite reflectivity from the CTRL and PGW simulations was used to calculate the frequency of occurrence in seven reflectivity ranges. Differences between the CTRL and PGW results in MJ show widespread decreases in weak 0–20 dBZ echoes over the continental US and decreases over the US Great Plains region of weak to moderate echoes (0–40 dBZ). Increases in the Pacific Northwest and Canada for moderate to intense 20–50 dBZ reflectivities indicate an enhanced convective population supported by the northward expansion of precipitation and precipitable water results discussed previously. Widespread increases in strong convective echoes (50–70 dBZ) over the entire continental US and Canada agree with previous studies in this region that demonstrated that more extreme precipitation events will occur in a warmer climate (Prein et al. 2016). However, the corresponding broad decrease in weak to moderate convection over the US indicates a shifting convective population.

An examination of the convective population in late summer shows a similar overall result, with decreases in the frequency of weak to moderate reflectivity and increases in strong to extreme reflectivity values over the US. One notable difference in JA compared to MJ is the increase in the occurrence of convection at all reflectivity ranges in the western US, possibly indicating more summertime convection over the Rockies and southwestern US. Increases in all reflectivity ranges is also noted along the Gulf Coast, possibly indicating enhanced tropical convection or land-sea breeze circulations, but further analysis is beyond the scope of the current study. In contrast, the US Great Plains shows a decreasing convective population in an expanded range (0–50 dBZ) compared to MJ. This decrease may be partially attributed to the warm bias (Liu et al. 2016) that results in too few mesoscale convective systems in this region in late summer (Prein et al. 2017), and may also be related to a general loss of soil moisture in the central US due to enhanced evapotranspiration in a warmer climate (Cook et al. 2015). Notable decreases in the weak to moderate convective population (0–50 dBZ) over the Gulf of Mexico and the Atlantic Ocean indicate less oceanic convection in the PGW simulation. Thus, from the analysis of the convective populations in both MJ and JA, a general shift in the convective population is observed in a future climate with more extreme events and fewer weak to moderate events over most of the US and surrounding oceans.

Given that the convective population may shift in a warmer climate, an investigation of the changing thermodynamic environments supporting convection in a current vs. future climate was conducted. Mixed-layer convective available potential energy (MLCAPE) and CIN are used to diagnose general changes in the energy available for convection

and the energy inhibiting convection, respectively. In MJ, both MLCAPE and CIN increase in magnitude in the PGW simulations downstream of the Rockies, with the largest increases occurring directly downstream of the mountains. A similar thermodynamic analysis for the late summer shows a similar pattern of increased MLCAPE and CIN over most of the continental US and surrounding oceans. However, given the warmer temperatures during the summer, the increases in both MLCAPE and CIN are more widespread than in MJ, including over the Rocky Mountains, Canada, and western Mexico. All 23 sounding stations examined in this study showed increases in the magnitude of both MLCAPE and CIN and are consistent with the bulk thermodynamic results. Specifically looking at the US Great Plains region, comparisons between MLCAPE and CIN values show that in the PGW simulation, the thermodynamic environments expand to higher magnitudes of both MLCAPE and CIN compared to the current climate especially in MJ and support the shifting convective population results.

Numerous previous studies have suggested that CAPE will increase in a future climate (Trapp et al. 2007, 2009; Muller et al. 2011; Diffenbaugh et al. 2013; Brooks 2013; Igel et al. 2013; Lackmann 2013; Singh and O’Gorman 2013; Gensini and Mote 2014; Trapp and Hoogewind 2016; Romps 2016) and are supported by these results, however a corresponding increase in CIN acts as a balancing force to shift the convective population across the US and surrounding oceans. Enhanced energy inhibiting convection results in a decreased frequency of weak to moderate storms and an increase in strong to extreme storms. If the parcels are subjected to strong lifting and can break through the stronger capping inversion, more vigorous updrafts can be expected given the increase in MLCAPE. However, a larger proportion of the parcels will not have enough external lifting to break the stronger capping inversion and thus the weak to moderate storms will be suppressed compared to the current climate. The modulation of the convective population by thermodynamic changes is most relevant over the continental US east of the Rocky Mountains and over the Gulf of Mexico and Atlantic Ocean.

An idealized investigation of fundamental changes in the thermodynamic environment in various climate states was conducted by using the Weisman and Klemp (1982) sounding and systematically changing the temperature profile (± 5 °C), while keeping relative humidity constant. Results from this study indicate that when temperature is increased, both MLCAPE and CIN increase in magnitude from a simple shift in temperature, while the opposite is true for decreased temperatures. This relationship holds for every degree of warming and cooling in this experiment showing that even in the absence of variations in synoptic and mesoscale conditions, a warmer climate will provide greater energy available for convection and greater energy

inhibiting convection. Thus, the results from the idealized thermodynamic experiments strongly support the thermodynamic environment results from this study and indicate a fundamental reason why the changes in MLCAPE and CIN are uniformly positive in a future climate.

This study presented an analysis of the changes in the mean and diurnal precipitation, frequency of high precipitable water values, the spectrum of weak to strong convection, and the thermodynamic environments supporting such changes in a future climate. A shift in the convective population to fewer weak to moderate storms and more strong to extreme storms is supported by increased MLCAPE and CIN. The balance between stronger MLCAPE and CIN may ultimately determine the character of the convective population across the US and beyond and should be considered in other regional climate studies around the world.

Acknowledgements The authors thank three anonymous reviewers for their comments and suggestions, which have improved this manuscript. This study was partially conducted while Kristen Rasmussen and Andreas Prein were supported by the National Center for Atmospheric Research (NCAR) Advanced Study Program. NCAR is sponsored by the National Science Foundation (NSF). The authors would like to thank the team of scientists in the Research Applications Lab (RAL) at NCAR for conducting the high-resolution convection-permitting climate simulations used in this study. The CONUS simulations are available on Yellowstone/Cheyenne and will soon be available on RDAS through the National Center for Atmospheric Research.

Open Access This article is distributed under the terms of the Creative Commons Attribution 4.0 International License (<http://creativecommons.org/licenses/by/4.0/>), which permits unrestricted use, distribution, and reproduction in any medium, provided you give appropriate credit to the original author(s) and the source, provide a link to the Creative Commons license, and indicate if changes were made.

References

- Allen MR, Ingram WJ (2002) Constraints on future changes in climate and the hydrologic cycle. *Nature* 419:224–232
- Ban N, Schmidli J, Schär C (2015) Heavy precipitation in a changing climate: does short-term summer precipitation increase faster? *Geophys Res Lett* 42:1165–1172
- Bengtsson L, Hodges KI, Roeckner E (2006) Storm tracks and climate change. *J Clim* 19:3518–3543
- Bohnen CF, Albrecht BA (1998) *Atmospheric thermodynamics*. Oxford University Press, Oxford
- Bony S, Dufresne JL, Le Treut H, Morcrette JJ, Senior C (2004) On dynamic and thermodynamic components of cloud changes. *Clim Dyn* 22:71–86
- Brooks HE (2013) Severe thunderstorms and climate change. *Atmos Res* 123:129–138
- Carbone R, Tuttle J (2008) Rainfall occurrence in the US warm season. The diurnal cycle. *J Clim* 21:4132–4146. <https://doi.org/10.1175/2008JCLI2275.1>
- Carlson TN, Benjamin SG, Forbes GS, Li Y-F (1983) Elevated mixed layers in the regional severe storm environment: conceptual model and case studies. *Mon Weather Rev* 111:1453–1474

- Chan SC, Kendon EJ, Fowler HJ, Blenkinsop S, Roberts NM, Ferro CAT (2014) The value of high-resolution Met Office regional climate models in the simulation of multi-hourly precipitation extremes. *J Clim* 27:6155–6174
- Cook BI, Ault TR, Smerdon JE (2015) Unprecedented 21st century drought risk in the American Southwest and Central Plains. *Sci Adv* 1:e1400082
- Craven J, Jewell R, Brooks H (2002) Comparison between observed convective cloud-base heights and lifting condensation level for two different lifted parcels. *Weather Forecast* 17:885–890
- Dai A, Giorgi F, Trenberth KE (1999) Observed and model-simulated diurnal cycles of precipitation over the contiguous United States. *J Geophys Res* 104:6377–6402
- Del Genio AD, Kovari W (2002) Climatic properties of tropical precipitating convection under varying environmental conditions. *J Clim* 15:2597–2615
- Deser C, Phillips A, Bourdette V, Teng H (2012) Uncertainty in climate change projections: the role of internal variability. *Clim Dyn* 38:527–546
- Dhuria HL, Kyle HL (1990) Cloud types and the tropical earth radiation budget. *J Clim* 3:1409–1434
- Diffenbaugh NS, Scherer M, Trapp RJ (2013) Robust increases in severe thunderstorm environments in response to greenhouse forcing. *Proc Natl Acad Sci* 110:16361–16366
- Doswell CA III (1985) The operational meteorology of convective weather. Vol II: storm scale analysis. NOAA Tech. Memo. ERL ESG-15, p 240 [NTIS PB85-226959.]
- Fritsch JM, Kane RJ, Chelius CR (1986) The contribution of mesoscale convective weather systems to the warm season precipitation in the United States. *J Clim Appl Meteorol* 25:1333–1345
- Geerts B, Parsons D, Ziegler C, Weckwerth T, Turner D, Wurman J, Kosiba K, Rauber R, McFarquhar G, Parker M, Schumacher R, Coniglio M, Haghi K, Biggerstaff M, Klein P, Gallus W, Demoz B, Knupp K, Ferrare R, Nehrir A, Clark A, Wang S, Hanesiak J, Pinto J, Moore J (2016) The 2015 plains elevated convection at night (PECAN) field project. *Bull Am Meteorol Soc*. <https://doi.org/10.1175/BAMS-D-15-00257.1>
- Gensini VA, Mote TL (2014) Estimations of hazardous convective weather in the United States using dynamical downscaling. *J Clim* 27:6581–6589
- Gensini VA, Mote TL (2015) Downscaled estimates of late 21st century severe weather from CCSM3. *Clim Change* 129:307–321
- Hansen J, Sato M, Ruedy R (1997) Radiative forcing and climate response. *J Geophys Res Atmos* 102:6831–6864
- Hara M, Yoshikane T, Kawase H, Kimura F (2008) Estimation of the impact of global warming on snow depth in Japan by the pseudo-global warming method. *Hydrol Res Lett* 2:61–64
- Hartmann DL, Michelsen ML (1993) Large-scale effects on regulation of tropical sea surface temperature. *J Clim* 6:2049–2062
- Hartmann DL, Ockert-Bell ME, Michelsen ML (1992) The effect of cloud type on Earth's energy balance: global analysis. *J Clim* 5:1281–1304
- Hartmann DL, Moy LA, Fu Q (2001) Tropical convection and the energy balance at the top of the atmosphere. *J Clim* 14:4495–4511
- Hawkins E, Sutton R (2011) The potential to narrow uncertainty in projections of regional precipitation change. *Clim Dyn* 37:407–418
- Held IM, Soden BJ (2006) Robust responses of the hydrological cycle to global warming. *J Clim* 19:5686–5699
- Hobbs PV (1993) *Aerosol-cloud-climate interactions*, vol 54. Academic Press, Cambridge
- Hohenegger C, Brockhaus P, Schär C (2008) Towards climate simulations at cloud-resolving scales. *Meteorol Z* 17:383–394
- Hong S-Y, Noh Y, Dudhia J (2006) A new vertical diffusion package with an explicit treatment of entrainment processes. *Mon Weather Rev* 134:2318–2341. <https://doi.org/10.1175/MWR3199.1>
- Houze RA Jr, Rasmussen KL, Zuluaga MD, Brodzik SR (2015) The variable nature of convection in the tropics and subtropics: a legacy of 16 years of the tropical rainfall measuring mission satellite. *Rev Geophys* 53. <https://doi.org/10.1002/2015RG000488>
- Iacono MJ, Delamere JS, Mlawer EJ, Shephard MW, Clough SA, Collins WD (2008) Radiative forcing by long-lived greenhouse gases: calculations with the AER radiative transfer models. *J Geophys Res*. <https://doi.org/10.1029/2008JD009944>
- Igel MR, van den Heever SC, Stephens GL, Posselt DJ (2013) Convective-scale responses of a large-domain, modeled tropical environment to surface warming. <https://doi.org/10.1002/qj.2230>
- Kawase H, Yoshikane T, Hara M, Kimura F, Yasunari T, Ailikun B, Ueda H, Inoue T (2009) Intermodel variability of future changes in the Baiu rainband estimated by the pseudo global warming downscaling method. *J Geophys Res* 114:D24110. <https://doi.org/10.1029/2009JD011803>
- Kendon EJ, Roberts NM, Senior CA, Roberts MJ (2012) Realism of rainfall in a very high resolution regional climate model. *J Clim* 25:5791–5806
- Kendon EJ, Roberts NM, Fowler HJ, Roberts MJ, Chan SC, Senior CA (2014) Heavier summer downpours with climate change revealed by weather forecast resolution model. *Nat Clim Change* 4:570–576
- Klein SA, Hartmann DL (1993) The seasonal cycle of low stratiform clouds. *J Clim* 6:1587–1606
- Kröner N, Kotlarski S, Fischer E, Lüthi D, Zubler E, Schär C (2016) Separating climate change signals into thermodynamic, lapse-rate and circulation effects: theory and application to the European summer climate. *Clim Dyn*. <https://doi.org/10.1007/s00382-016-3276-3>
- Lackmann GM (2013) The South-Central US flood of May 2010: present and future. *J Clim* 26:4688–4709
- Le Treut H, McAvaney B (2000) A model intercomparison of equilibrium climate change in response to CO2 doubling. Note du Pôle de Modélisation de l'IPSL, 2000
- Lenderink G, van Meijgaard E (2010) Linking increases in hourly precipitation extremes to atmospheric temperature and moisture changes. *Environ Res Lett* 5:025208. <https://doi.org/10.1088/1748-9326/5/2/025208>
- Liu C, Allan RP (2013) Observed and simulated precipitation responses in wet and dry regions 1850–2100. *Environ Res Lett* 8(3):034002. <https://doi.org/10.1088/1748-9326/8/3/034002>
- Liu C, Ikeda K, Rasmussen R, Barlage M, Newman AJ, Prein AF, Chen F, Chen L, Clark M, Dai A, Dudhia J, Eidhammer T, Gochis D, Gutmann E, Kurkute S, Li Y, Thompson G, Yates D (2016) Continental-scale convection-permitting modeling of the current and future climate of North America. *Clim Dyn*. <https://doi.org/10.1007/s00382-016-3327-9>
- Lucarini V, Fraedrich K, Lunkeit F (2010) Thermodynamics of climate change: generalized sensitivities. *Atmos Chem Phys* 10:9729–9737
- Mahoney K, Alexander M, Scott JD, Barsugli J (2013) High-resolution downscaled simulations of warm-season extreme precipitation events in the Colorado front range under past and future climates. *J Clim* 26:8671–8689
- Morcrette C, Petch J, Ma H-Y, Klein S, Xie S (2013) Clouds above the United States and errors at the surface (CAUSES). http://asr.science.energy.gov/meetings/fall-workinggroups/2013/presentations/causes_for_mc3e_breakout.pdf. Accessed 1 Oct 2015
- Muller CJ, O'Gorman PA, Back LE (2011) Intensification of precipitation extremes with warming in a cloud-resolving model. *J Clim* 24:2784–2800
- Niu GY et al (2011) The community Noah land surface model with multiparameterization options (Noah-MP): 1. Model description and evaluation with local-scale measurements. *J Geophys Res*. <https://doi.org/10.1029/2010JD015139>

- O’Gorman PA, Schneider T (2009) The physical basis for increases in precipitation extremes in simulations of 21st-century climate change. *Proc Natl Acad Sci* 106(35):14773
- Pall P, Allen MR, Stone DA (2007) Testing the Clausius–Clapeyron constraint on changes in extreme precipitation under CO₂ warming. *Clim Dyn* 28:351–363
- Pan L-L, Chen S-H, Cayan D, Lin M-Y, Hart Q, Zhang M-H, Liu Y, Wang J (2011) Influences of climate change on California and Nevada regions revealed by a high-resolution dynamical downscaling study. *Clim Dynam* 37:2005–2020
- Prein AF et al (2015) A review on regional convection-permitting climate modeling: demonstrations, prospects, and challenges. *Rev Geophys* 53:323–361
- Prein AF, Rasmussen RM, Ikeda K, Liu C, Clark MP, Holland GJ (2016) On the future intensification of hourly precipitation extremes. *Nat Clim Change*. <https://doi.org/10.1038/nclimate3168>
- Prein AF, Liu C, Ikeda K, Bullock R, Rasmussen RM, Holland GJ, Clark M (2017) Simulating convective storms: a new benchmark for climate modeling. *Clim Dyn*
- Rasmussen KL, Houze RA Jr (2011) Orographic convection in South America as seen by the TRMM satellite. *Mon Weather Rev* 139:2399–2420
- Rasmussen KL, Houze RA Jr (2016) Convective initiation near the Andes in subtropical South America. *Mon Weather Rev* 144:2351–2374
- Rasmussen RM et al (2011) High-resolution coupled climate runoff simulations of seasonal snowfall over Colorado: a process study of current and warmer climate. *J Clim* 24:3015–3048
- Rasmussen KL, Zuluaga MD, Houze RA Jr (2014a) Severe convection and lightning in subtropical South America. *Geophys Res Lett* 41:7359–7366
- Rasmussen RM et al (2014b) Climate change impacts on the water balance of the Colorado headwaters: high-resolution regional climate model simulations. *J Hydrometeorol* 15:1091–1116
- Rasmussen KL, Chaplin MM, Zuluaga MD, Houze RA Jr (2016) Contribution of extreme convective storms to rainfall in South America. *J Hydrometeorol* 17:353–367
- Romps DM (2016) Clausius–Clapeyron scaling of CAPE from analytical solutions to RCE. *J Atmos Sci* 73:3719–3737
- Romps DM, Seeley JT, Vollaro D, Molinari J (2014) Projected increase in lightning strikes in the United States due to global warming. *Science* 346:851–854. <https://doi.org/10.1126/science.1259100>
- Rotunno R, Klemp JB, Weisman ML (1988) A theory for strong, long-lived squall lines. *J Atmos Sci* 45:463–485
- Sato T, Kimura F, Kitoh A (2007) Projection of global warming onto regional precipitation over Mongolia using a regional climate model. *J Hydrol* 333:144–154
- Schär C, Frie C, Lüthi D, Davies HC (1996) Surrogate climate-change scenarios for regional climate models. *Geophys Res Lett* 23:669–672
- Seager R, Ting M, Held I, Kushnir Y, Lu J, Vecchi G, Huang H-P, Harnik N, Leetmaa A, Lau N-C, Li C, Velez J, Naik N (2007) Model projections of an imminent transition to a more arid climate in southwestern North America. *Science* 316(5828):1181–1184
- Seeley JT, Romps DM (2015) Why does tropical convective available potential energy (CAPE) increase with warming? *Geophys Res Lett* 42:10429–410437. <https://doi.org/10.1002/2015GL066199>
- Sheffield J, Wood EF (2008) Projected changes in drought occurrence under future global warming from multi-model, multi-scenario, IPCC AR4 simulations. *Clim Dyn* 31:79–105
- Shepherd TG (2014) Atmospheric circulation as a source of uncertainty in climate change projections. *Nat Geosci* 7:703–708
- Singh MS, O’Gorman PA (2013) Influence of entrainment on the thermal stratification in simulations of radiative-convective equilibrium. *Geophys Res Lett* 40:4398–4403
- Stephens G, Webster P (1981) Clouds and climate: sensitivity of simple systems. *J Atmos Sci* 38:235–247
- Thompson G, Eidhammer T (2014) A study of aerosol impacts on clouds and precipitation development in a large winter cyclone. *J Atmos Sci* 71:3636–3658
- Trapp R, Hoogewind K (2016) The realization of extreme tornadic storm events under future anthropogenic climate change. *J Clim* 29:5251–5265
- Trapp RJ, Diffenbaugh NS, Brooks HE, Baldwin ME, Robinson ED, Pal JS (2007) Changes in severe thunderstorm environment frequency during the 21st century caused by anthropogenically enhanced global radiative forcing. *Proc Natl Acad Sci* 104:19719–19723
- Trapp RJ, Diffenbaugh NS, Gluhovsky A (2009) Transient response of severe thunderstorm forcing to elevated greenhouse gas concentrations. *Geophys Res Lett* 36:L01703. <https://doi.org/10.1029/2008GL036203>
- Trapp RJ, Robinson ED, Baldwin ME, Diffenbaugh NS, Schwedler BRJ (2010) Regional climate of hazardous convective weather through high-resolution dynamical downscaling. *Clim Dyn* 37:677. <https://doi.org/10.1007/s00382-010-0826-y>
- Trenberth KE, Dai A, Rasmussen RM, Parsons DB (2003) The changing character of precipitation. *Bull Am Meteorol Soc* 84:1205–1217
- Weisman ML, Klemp JB (1982) The dependence of numerically simulated convective storms on vertical wind shear and buoyancy. *Mon Weather Rev* 110:504–520
- Zipser EJ, Liu C, Cecil DJ, Nesbitt SW, Yorty DP (2006) Where are the most intense thunderstorms on Earth? *Bull Am Meteorol Soc* 87:1057–1071
- Zuluaga MD, Houze RA Jr (2015) Extreme convection of the near-equatorial Americas, Africa, and adjoining oceans as seen by TRMM. *Mon Weather Rev* 143:298–316